Poster Program

Display 13:30-13:40 Obligation 13:40-14:20

P01 3D Conformational Analysis of Tetrapod DNA with Small Angle X-ray Scattering
Shunsuke Sakamoto (The University of Kitakyushu)

P02 Existence of Liquid Crystalline Domain in Intercellular Lipid Matrix of Stratum Corneum and Its Role in Barrier Function
Ichiro Hatta (Nagoya Industrial Science Research Institute)

P03 Structural analysis of sodium colistin methanesulfonate having ring structure
Aya Okura (The University of Kitakyushu)

P04 The Latest Model MIRRORCLE-400 High Brilliant Tabletop SLS
Hironari Yamada (Ritsumeikan University)

P05 Analysing the Stracture of Micelle Formed From Cationic Calix[4]arene Modified Dendron in Hydrophilic Group
Genki Kubo (The University of Kitakyushu)

P06 Synthesis and Characterization of Micelles Comprised of Calix[4]arene Amphiphilies Bearing Choline Phosphate and the Cell Recognition by PC-CP Interaction
Shota Fujii (Kyushu University)

P07 Structural Analysis of Micelles Formed by Calix[4]arene lipids bearing Quaternized Amine
Shinpei Yamada (The University of Kitakyushu)

P08 Relaxation process of the thermal phase transition in stratum corneum intercellular lipids studied by Synchrotron X-ray Diffraction
Tomohiro Imai (Kwansei Gakuin University)

P09 Characterization of Sugar-Bearing Micelles for Targeting Drug Delivery
Mizuha Sakashita (The university of Kitakyushu)

P10 Micellar Structure of an Amphiphilic Alternating Copolymer in Aqueous Medium
Takahiro Sato (Osaka University)

P11 Analysis of cationic dendrimer's structure using Small angle X-ray scattering
Takuma Minami (The University of Kitakyushu)

P12 Conformation and Association Behavior of Single-Stranded DNA in Aqueous Solution
Hiroki Yamamura (Osaka University)

P13 Local Conformation and Intermolecular Interactions of Rigid Cyclic Amylose Carbamate Derivatives
Ken Terao (Osaka University)

P14 Colloidal Dispersion of a Thermosensitive Block Copolymer in Water
Masaaki Kondo (Osaka University)

P15 Temperature changes in molecular conformation and intermolecular interactions of polydialkyl silanes in solution
Jiang Xinyue (Osaka University)

P16 Mannose-bearing Micelles for Targeting DDS and its Structure
Ichiki Fukuda (The University of Kitakyushu)

P17 Orientation and Distribution of Intercellular Lipid Domains in Pig Stratum Corneum
Shiori Kakinoki (Tokyo Metropolitan University)

P18 Analysis of Structural Change in pH-responsive Polymer Micelle with Anomalous Small angle X-ray scattering
Masaki Kinoshita (The University of Kitakyushu)

P19 Methionine adsorption on Au nanoparticle surface fabricated by solution plasma method compared with cysteine adsorption
Shinya Yagi (Nagoya University)

P20 Adsorption reaction between biomolecules and gold nanoparticles prepared by solution plasma method
Chie Tsukada (Nagoya University)

P21 Anomalous diffusion of polystyrene grafted nanoparticles dispersed in polystyrene matrix studied by X-ray photon correlation spectroscopy
Taiki Hoshino (JST-ERATO Takahara Softinterfaces, RIKEN/SPring-8)

P22 Structure analysis of associating structure of amphiphilic ABn-type polymer with small-angle X-ray scattering
Daisuke Kugimoto (The university of Kitakyushu)

P23 Upgrade and Promotion of Industrial Use of Small Angle X-ray Scattering Beamlines at the Photon Factory
Hideaki Takagi (Photon Factory, Institute of Materials Structure Science, KEK)

P24 Application of SR-XRF and XAFS for the trace element analysis contained in histopathological specimens
Motohiro Uo (Tokyo Medical and Dental University)

P25 Influence of alkyl chain length of calix[4]arene-based cationic lipid for transfection efficiency
Koichi Nishina (The university of Kitakyushu)

P26 RIKEN Small Angle X-ray Scattering Beamline (BL45XU) at SPring-8
Takaaki Hikima (RIKEN SPring-8 Center)

P27 Induced Circular Dichroism for Micelles of Sugar-Calix[4]arene and SAXS
Shunsuke Sakamoto (The University of Kitakyushu)

3D Conformational Analysis of Tetrapod DNA with Small Angle X-ray Scattering

Shunsuke Sakamoto[1], Yusuke Sanada[1,2], Tadashi OKOBIRA[2,3], Makiya NISHIKAWA[4], Naoto YAGI[2,5] and Kazuo Sakurai[1,2]

[1]Department of Chemistry & Biochemistry, the University of Kitakyushu, [2]JST-CREST, [3]Ariake National College of Technology, [4] Kyoto University, [5]JASRI/SPring-8
[1]1-1 Hibikino, Wakamatsu-ku, Kitakyushu, Fukuoka 808-0135, Japan.
E-mail: t2mab009@eng.kitakyu-u.ac.jp

Introduction

DNAs with defined sequences conform tetrapod shape in the aqueous solution. Small-angel X-ray scattering was carried out for 2 kinds of DNA tetrapodnas. One has the complementary sequence for all base pairs (A), and the other has short non-complementally parts at the center of the DNA tetrapodna (B). SAXS profile at low q region can be explained with a simple tetrapod model with 4 arms. The tetrapodna B has relatively long arm, that mean the tetrapod B took a spread structure compared with tetrapod A. We think it is because of instability of the DNA tetrapodna with short non-complementally parts.

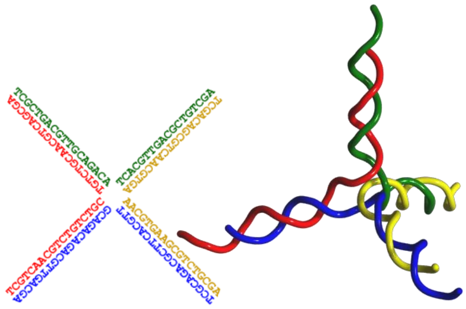

Figure 1. An example of the sequence of DNA tetrapodna and its schematic picture of a tetrapodna.

Experiments

All ODNs used were purchased from Integrated DNA Technologies, Inc. (Coralville, IA, USA) We constructed four tetrapodna DNA samples from four appropriate ODNs. Samples were packed into a quartz capillary cell with the diameter of 2 mm. The incident X-ray wavelength λ was fixed at 1.0 Å, and we measure scattering with two sample-to-detector distances (2.25 and 1.65 m) and combined two profiles afterward to obtain I(q) vs q plots, where I(q) and q are the excess scattering intensity and the absolute value of the scattering vector.

Results and Discussions

Figure 2 shows the SAXS profiles for the tetrapod DNAs. The code A means they included 0 base pairs of non-complementally sequences. The code B means that this tertapodna has eight mismatched base-pairs. While all of them showed similar patterns which are typical for isolated scattering particles, there are small but significant differences observed between A and B. In the range of 0.3 nm^(-1)<q<0.8 nm^(-1), I(q) for B was deviated downward from the other samples. In the range of 3.0 nm^(-1)<q corresponding to the DNA fingerprint region, all of the samples had a diffraction peak at q=4.5 nm^(-1) but the peak width of B was broader than the others.

The diffraction peaks at q=4.5 nm^(-1) in the finger print region can be ascribed to the atomic structures for the typical B-type DNA. As mentioned above, the peak width of B was larger than the others, ascribing to less ordered structures or/and smaller amount of the ordered structures than the others. This fact is relating that B has a several mismatched pairs (thus single strand).

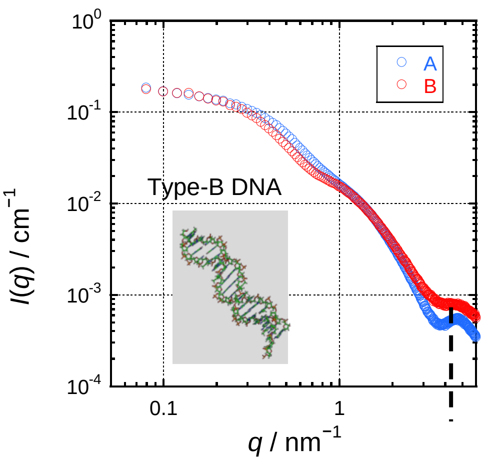

Figure 2. SAXS profiles of tetrapod DNA A and B, and Type-B DNA.

Acknowledgment

This work is financially supported by JST CREST program and all SAXS measurements were carried out at SPring-8 BeamLine40B2 (2012B1252, 2013A1594).

Reference

[1] Makiya Nishikawa, Mitsuhiro Matono, Sakulrat Rattanakiat, Nao Matsuoka and Yoshinobu Takakura. *Immunology,* **2008**, 124, 247-255.

Existence of Liquid Crystalline Domain in Intercellular Lipid Matrix of Stratum Corneum and Its Role in Barrier Function

Ichiro Hatta[1], Hiromitsu Nakazawa[2], and Noboru Ohta[3]

[1]Nagoya Industrial Science Research Institute, [2]Kwansei Gakuin University, [3]JASRI/Spring-8
E-mail: hatta@nisri.jp

Introduction

The modification of the barrier function of stratum corneum (SC) by applying organic solvents is an important subject in pharmaceutics and in cosmetics. A variety of organic solvents has been used for the structure alternation that promotes efficiently permeation and solubility. It has been pointed out that when the organic solvents are applied to skin, lipids in SC are extracted markedly by chloroform/methanol mixture, but slightly by acetone and much slightly by ethanol. As a moderate basic solvent we pay our attention to the effect of ethanol and acetone on the structure of SC. In the present study we measured the detailed behavior of the change of the X-ray diffraction profiles by treating SC with the solvents. Based upon the measurement we propose the existence of the liquid crystalline domain in the intercellular lipid matrix in which the same components of the lipids as in the order domains are contained and work as a reservoir in reconstitution of the order domains.

Experimental

To detect the successive minute structural change in human SC after applying organic solvent to the SC, we have developed a sample cell for the high-sensitive wide-q-range X-ray diffraction measurement [1]. Using this method the X-ray scattering profiles were observed in the range from S=0.05-4.0 nm^{-1} as a function of time on applying either ethanol or acetone, here $S=(2/\lambda)\sin\theta$, where λ is wavelength of the X-ray and 2θ is scattering angle. After the human SC was soaked in the solvents, the successive changes of the diffraction profiles were observed up to about 10000 s, afterwords the solutions surrounding the SC were removed, then the SC was dried for about 10 h so as to exhaust the solvents from the SC and at last the resultant diffraction profiles were observed.

Results and Discussion

The obtained results indicate that the structure change takes place in the lamellar and the hydrocarbon-chain packing. The sapacing of the short lamellar structure in the human SC increased with time by incorporating the solvents, ethanol and acetone, conversely decreased down to lower than the intitial one when the solvents were exhausted from the SC, and the integrated intensity decreased with time, conversely increased markedly when the sovlents were removed. The sapcing of the hydrocarbon-chain packing structure at S=2.4 nm^{-1} did not change markedly before and after the treatment of the solvents, and also the integrated intensity also did not change markedly with time on applying the solvents, but the integrated intensity became bigger than the initial one when the solutions were exhausted from the SC.

The above behavior takes place in the same manner when ethanol and acetone were applied., although the effect is slightly strong in the acetone treatment. Therefore the extraction of the lipids is not so significant in these treatment. At present we take notice of the behavior of the hydrocarbon-chain packing structure. As shown in Fig. 1, when the solvents are applied to SC, the ratio of the hexagonal hydrocarbon-chain packing domain decreases from (a) to (b), and when the solvents are removed from SC, the hexagonal hydrocarbon- chain packing domain is reconsititGuted beyond before the treatment as shown in (c). This fact indicates that in the untreated SC there is the liquid crystalline state which has potential to construct the hexagonal hydrocarbon- chain packing structure when some disruption takes place in SC.

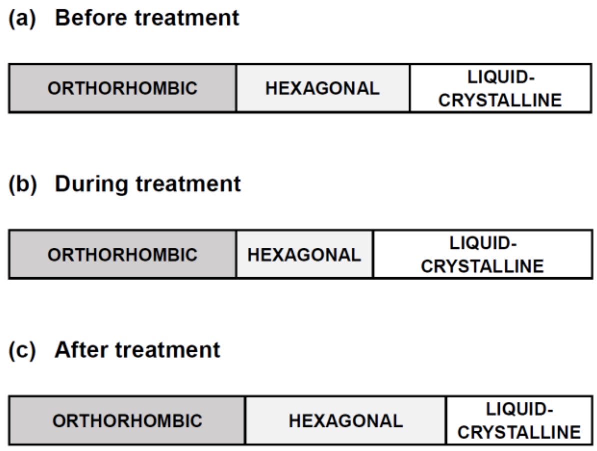

Fig. 1 The ratio of the domains of orthorhombic, hexagonal, and liquid crystalline hydrocarbon-chain packing, whose diffraction peaks take place at S=2.4 and 3.7 nm^{-1}, S=2.4 nm^{-1}, and S~2.1 nm^{-1}, respectively, (a) before, (b) during and (c) after the treatment of either ethanol or acetone.

Reference

1) I. Hatta, H. Nakazawa, Y. Obata, N. Ohta, K. Inoue and N. Yagi, Chem. Phys. Lipids **163** (2010) 382.

P03

Structural analysis of sodium colistin methanesulfonate having ring structure

Aya Okura, Masaki Kinoshita, Daisuke Kugimoto, Isamu Akiba

Department of Chemistry & Biochemistry, The University of Kitakyushu, Kitakyushu, Japan

1-1 hibikino, Wakamatsu, Kitakyushu-city, Fukuoka, Japan

E-mail : u3maa001@eng.kitakyu-u.ac.jp

Introduction

Sodium colistin methanesulfonate (CMS) is a biosurfactant and an amphiphiplic oligopeptide having ring structure with diameter of about 1 nm as shown in Fig. 1. Recently, the CMS is focused because it has a bacteria resistance and a pharmacological activity to pseudomonas. However, fundamental properties, such as aggregating structures in solution and solution properties, of CMS have not been well understood. It is considered that a pharmacological activity of CMS is closely associated with its aggregating structures in aqueous solution. Therefore, it is significant important to understand aggregating structures of CMS in aqueous solution. Thus, in this study, we examine an association structure of CMS in aqueous solution by small-angle X-ray scattering (SAXS).

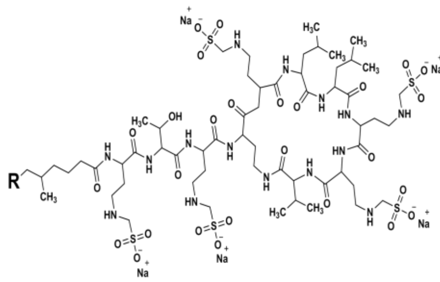

Fig.1. The structure of CMS.

Experiment

CMS was dissolved in water containing various amount of NaCl. Associating behavior of CMS in aqueous solution was evaluated from small-angle X-ray scattering (SAXS), dynamic light scattering (DLS), and field-flow fractionation combined with multi-angle light scattering (FFF-MALS). SAXS measurements were performed at BL-40B2 of SPring-8, Japan.

Results and Discussion

Fig.2 shows SAXS profiles of CMS in aqueous solution and in 14.2M NaClaq solution. SAXS profile of aqueous solution of CMS shows a broad peak around 1 nm^{-1}. On the contrary, the peak is disappeared in the SAXS profile of CMS in 14.2M NaClaq solution. This means that the broad peak indicates interference between macroions of CMS aggregates and the interference is shielded by NaCl. Therefore, the SAXS profile of CMS in 14.2M NaClaq solution corresponds to form factor of CMS aggregates. The radius of gyration of CMS aggregates is estimated to 1.0 nm from Guinier plot for the SAXS profile.

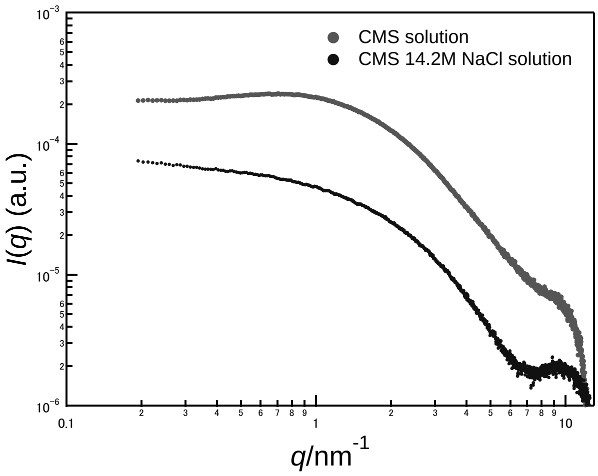

Fig.2. SAXS profiles of CMS in aqueous solution and CMS in 14.2M NaCl solution.

P04

The Latest Model MIRRORCLE-400 High Brilliant Tabletop SLS

Daisuke Hasegawa[2], Shuji Maeo[2], and Hironari Yamada[1,2]
[1]Ritsumeikan U, [2]Photon Production Laboratory Ltd.
1-1-1 Nojihigashi, Shiga
hironari@se.ritsumei.ac.jp

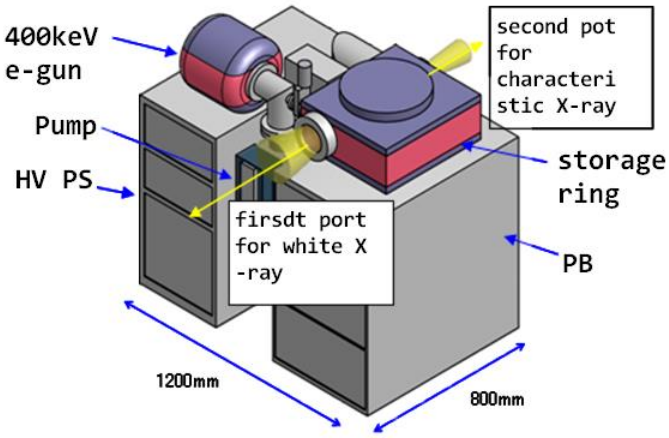

A synchrotron light source (SLS) is advantageous against an X-ray tube and other X-ray sources by its brightness, contentious spectrum, and small focus size. By the same reason a MIRRORCLE tabletop synchrotron light source is advantageous. MIRRORCLE is even favoured by its laboratory size, the focus point size less than 10 μm, the X-ray energy range up to MeV order, and wide radiation angular distribution in the range of several 100 mrad. Due to these features MIRRORCLE can provide applications such as a magnified phase contrast X-ray imaging, a fine resolution X-ray CT for a heavy mechanism, a small angle scattering and EXAFS. Even recently we could demonstrate a residual stress measurement using around 100keV X-rays on a steal at deep inside up to 5 mm.

A week point of MIRRORCLE was, however, there in its lower X-ray flux compared with SLS. Therefore we developed a new technology which improves the radiation power more than 100 times. A beam injection is the key technology of MIRRORCLE. So we introduced a multi-pulse or a continuous wise resonance injection method. We report in this paper how we could upgrade the radiation power to 10^13 brilliance/s, mm^2, mrad^2, 0.1%b.w.

The latest model is named MIRRORCLE-400. A 400 keV DC accelerator is used instead of microtron pulse source and CW injection is carried out leading to 100 times more flux. The specification of this model is listed in the following table. Two ports are available. Characteristic X-rays are also available.

source size for line target	minimum 0.7 μm horizontally in FWHM and 1mm vertically
for sphear target	minimum 15 μm in any direction in FWHM
Sourcce to ample distance	100-150 mm variable
Photon density of port #1	more than 10^8 density(/sec/mrad^2/0.1% band width) (10^12 Brilliance)
	contentious spectrum ranging a from a few keV up to 400 keV
Photon density of port #2	more than 10^9 density(/sec/mrad^2/0.1% band width)(10^13 Brilliance)
	Characteristic X-ray (monochromatic X-ray energy is selectable by target)
Fan beam CT	Fan beam of 10-20 mm thickness and 1 rad spread is produced by a collimator.
	maximum sample size is 50 mm horizontally, no limit vertically.
	scanning speed is 1 sec/flame, 6 minutes/slice.
	space resolution is 0.7 μm
	Suitable port # can be selected by user.
	Detector pixel size is 5 μm.

P05

Analysing the Stracture of Micelle Formed From Cationic Calix[4]arene Modified Dendron in Hydrophilic Group

Genki Kubo[1], Hiroko Yamamoto[1], Shota Fujii[1], Yusuke Sanada[1, 2], Kazuo Sakurai[1,2]

[1]Department of Chemistry and Biochemistry, University of Kitakyushu, [2]JST-CREST

[1]1-1 Hibikino, Wakamatsu-ku, Kitakyushu, Fukuoka 808-0135, Japan.

E-mail: r0551015@eng.kitakyu-u.ac.jp

Introduction

An amphiphilic compounds are known to form micelles of various shapes in aqueous solutions. But micelles are generally polydisperse and aggregation number is not constant. Additionally, there is no report on monodisperse micelles. So far, in our laboratory, we newly synthesized the cationic calix[4]arene bearing amine in hydrophilic groups (denoted by CaL[4]C3,Figure.1). The micelles formed from CaL[4]C3 are formed a regular hexahedron structure monodisperse under acidic conditions. Further, the structure of the lipid micelles are varying substantially depending on the presence or absence of intramolecular electrostatic repulsion.

However, the relationship between the structure of the micelles and the size of the hydrophilic groups is not clear enough. In this study, we newly synthesized cationic calix[4]arene-based lipid having a dendron in hydrophilic group (denoted by PAMAM-CaL[4]C3, Figure.1). And, we analyze the structure of micelles formed from PAMAM-CaL[4]C3.

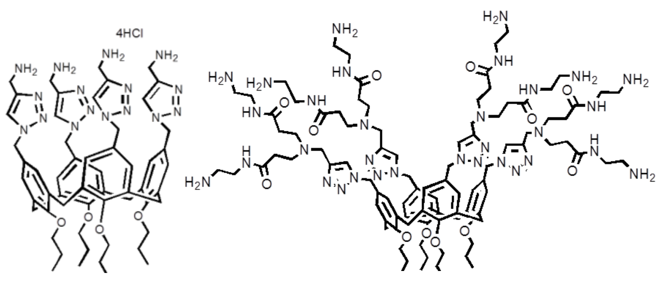

CaL[4]C3 PAMAM-CaL[4]C3

Figure.1 Chemical structure of CaL[4]C3&PAMAM-CaL[4]C3

Experiments

We synthesized a cationic calix[4] arene-based lipid. The PAMAM-CaL[4]C3.

SAXS(small angle X-ray scattering) measurements were performed at BL40B2 of SPring-8, Japan. An imaging plate (Rigaku R-AXIS VII) detector was placed at 1.0 m away from the sample. The sample concentration was 3.0 mg / mL and the solvent was water and methanol.

Results and Discussion

Figure.2 shows SAXS profiles of PAMAM-CaL[4]C3 in water and methanol. The results revealed that PAMAM-CaL[4]C3 is molecular dispersion in methanol. Percentage of water increases, begin to form spherical micelles. Finally, become only spherical micelles in water. We found the aggregation number of this micelle is 8 by absolute intensities of SAXS.

In this way, we reported the results of structural analysis of micelle formed from PAMAM-CaL[4]C3.

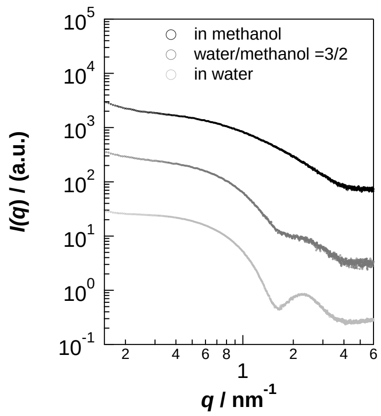

Figure.2 SAXS profile of PAMAM-CaL[4]C3 in water and methanol.

P06

Synthesis and Characterization of Micelles Comprised of Calix[4]arene Amphiphilies Bearing Choline Phosphate and the Cell Recognition by PC-CP Interaction

Shota Fujii[1], Koichi Nishina[3], Kazuo Sakurai[3], and Atsushi Takahara[1,2]

[1]Graduate School of Engineering and [2]Institute for Materials Chemistry and Engineering, Kyushu University, 744 Motooka, Nishi-ku, Fukuoka 819-0395, Japan,
[3]Department of Chemisty and Biochemistry, University of Kitakyushu, Hibikino, Kitakyushu 808-0135, Japan
E-mail: s-fujii@ms.ifoc.kyushu-u.ac.jp

Introduction

Cationic micelles are used in drug delivery system as an active targeting carrier. However, they interact non-specifically with negatively charged serum proteins via cation-anion interaction, which might induce high cytotoxicity. Thus, the development of non-cationic micelles as a vecetor has been strongly desired. To overcome this problem, we focused on preparation of non-cationic micelles.

So far, the chemical interaction between phosphoryl choline (PC) covering on biomembranes surface and choline phosphate (CP) has been reported.(1) As the PC-CP interaction does not related to a cation-anion interaction, the micelles bearing CP on the surface could become the novel vector. In this work, we synthesized new calix[4]arene lipids attached CP groups (denoted by CPCaL*n*, Figure 1) and investigated the interacton between the CP-micelles and biomembranes.

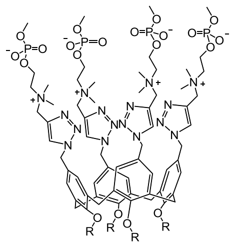

Figure 1. Chemical structure of CPCaL*n*.

Experiment

The CPCaL*n* were dissolved in 150 mM NaCl solution in all experiment. The micelle shape and its aggregation number were investigated with small angle X-ray scattering (SAXS) and light scattering coupled with field flow fractionation (FFF-MALS). A549 cell was used for evaluation of cell uptake. Fluorescence micelles comprised of CPCaL*n* and fluorescein-labelled lipid were prepared and it was seeded into the cells. After 6 h incubation at 37°C, the cells were washed with PBS, and then the cell uptake of CPCaL*n* micelles were observed with fluorescence microscope.

Result and Discussion

Figure 2 shows the SAXS profiles of the CPCaL3 and CPCaL6 micelles in 150 mM NaCl solution. The fitting curves were calculated with shape determining program. The resultant shapes determined from the fitting showed that both of CPCaL*n* micelles are spherical with 4-6 nm in diameter. In addition, CPCaL6 micelle is slightly strained compared to CPCaL3 micelle, and it looks like ellipsoidal shape. FFF-MALS results showed that the aggregation numbers of CPCaL*n* micelles are constant, which means that monodisperse micelles so called shape-persistent micelles were formed. (2)

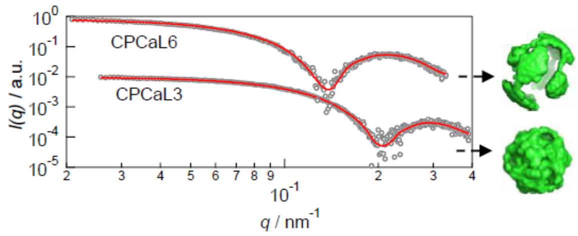

Figure 2. SAXS profiles of 1.0 mM CPCaL*n* micelles in 150 mM NaCl solution. The red solid line was fitted with shape determining program.

Figure 3 shows the results of the cell uptake on the basis of fluorescence observation. The cell uptake was observed in CP-micelles system, while PC-micelles did not penetrate into the cells. This indicates that the CP-micelles interact with biomembrane by PC-CP interaction. Furthermore, in comparison with CPCaL3 having shorter alkyl chains, CPCaL6 showed higher cell uptake. This also implies that the alkyl tails length is important for the interaction of CP-micelles with PC-biomembrane.

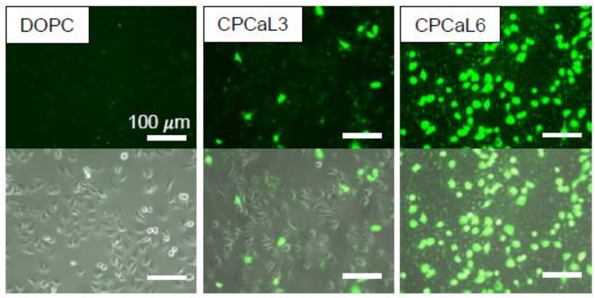

Figure 3. Observation of cellular uptake via fluorescence and phase-contrast microscopy. The upper side shows the fluorescence images and the lower side shows the fluorescence images merged with phase-contrast ones.

Reference

(1) Yu et al., *Nature Materials*, **2012**, *11*, 468–476.
(2) Fujii et al., *Langmuir*, **2012**, *28* (6), 3092–3101.

P07

Structural Analysis of Micelles Formed by Calix[4]arene lipids bearing Quaternized Amine

Shinpei Yamada[1], Yurika Kamibeppu[1], Shota Fujii[1], Yusuke Sanada[1,2], and Kazuo Sakurai[1,2]

[1]Department of Chemistry & Biochemistry, the University of Kitakyushu, [2]JST-CREST

[1]1-1 Hibikino, Wakamatsu-ku, Kitakyushu, Fukuoka 808-0135, Japan.

E-mail: r0551047@eng.kitakyu-u.ac.jp

Introduction

An amphipathic compound forms a micelle in water by self-aggregation. The inner side of micell is hydrophobicity. Therefore, medicines can be included there and these are expected as an application to DDS. But its detailed structure isn't revealed and its aggregation number is non-constant because micelle is generally polydispersion.

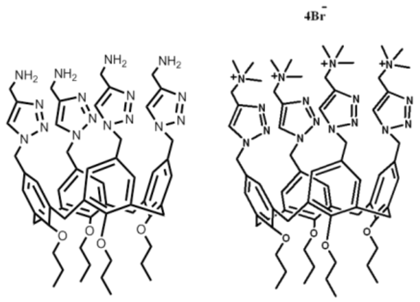

Cal3 QA

Figure1. chemical structures of Cal[4]C3(a) and QA(b)

We reported that calix[4]arene bearing amine in hydrophilic portion(Fig.1) form monodisperse micelles[1], but its condition was acidity. To use for DDS, it needs to become monodisperse in a neutral pH. We synthesized new amphiphilic calix[4]arene bearing quaternary amine(QA) and explored pH dependence of physiochemical characterization of QA by using of small-angle X-ray scattering(SAXS) in detail.

Experiments

We synthesized calix[4]arene bearing quaternary amine in hydrophilic portion. And, we analyzed the structure and pH dependence by SAXS. We decided the aggregation number of QA with Field Flow Fractionation (FFF) coupled with Malt Angle Light Scattering (MALS)

Results and Discussions

Figure3 shows the SAXS profiles of all samples at different pHs in the presence of 50 mM NaCl. This shows that QA is not pH-responsive structural changes. We used a core–shell sphere to fit the profiles at pH =8.0, and thus the data were fitted with a core–shell sphere model. Its diameter was about 1.9 nm. In addition, aggregation number of QA is 8 , and it was monodisperse. That is, because QA have electrostatic repulsion in neutral pH, we could make monodisperse micelles in neutral pH.

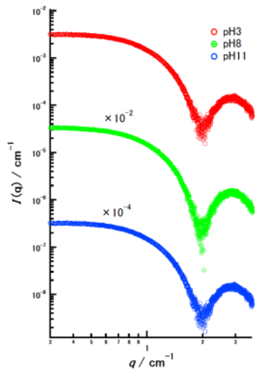

Figure3.SAXS profiles of pH-responsive structural changes of QA

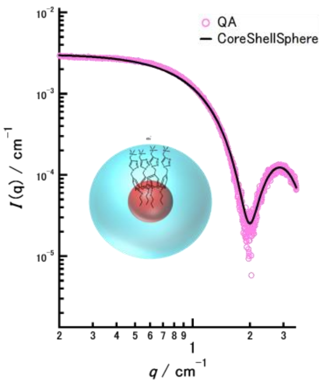

Figure3.SAXS profiles of core–shell sphere model and QA

Reference

[1] Shota Fujii, Yusuke Sanada, Tomoki Nishimura, Isamu Akiba, and Kazuo Sakurai , Naoto Yagi and Efstratios Mylonas ,*Langmuir*, **2012**, *28* (6),

P08

Relaxation process of the thermal phase transition in stratum corneum intercellular lipids studied by Synchrotron X-ray Diffraction

Tomohiro Imai, Hiromitsu Nakazawa, and Satoru Kato
Department of Physics, Graduate School of Science & Technology, Kwansei Gakuin University
2-1, Gakuen, Sanda, Hyogo 669-1337, Japan
t.imai@kwansei.ac.jp

Introduction

The major role of the stratum corneum (SC), the outermost layer of the human skin, is to work as a physicochemical barrier between inner body and outer environment. The lateral packing structure of the intercellular lipids has been reported to be involved in the barrier capability [1]. It is known that the intercellular lipids undergo an orthorhombic-to-hexagonal structural phase transition at 30-40°C [2]. We have previously described the detailed thermal phase behavior of the SC based on synchrotron x-ray and electron diffraction measurements [3, 4]. Since the orthorhombic-to-hexagonal transition takes place near the physiological temperature, the lipid packing structures must be affected by the temperature variation experienced in everyday life. Therefore, the hysteresis properties of the transition may be related to the barrier function of SC. In this study, we analysed the relaxation process of the thermal phase transition by synchrotron x-ray diffraction.

Experimental

The SC structural change with temperature was examined by wide-angle synchrotron x-ray diffraction (WAXD). Human skin SC samples were purchased from BIOPREDIC International (France) and used in the WAXD measurements. WAXD patterns were obtained from SC during heating and cooling between 25°C and 40°C.

Results

At room temperature, the WAXD patterns from SC showed the coexistence of sharp diffraction peaks from lipid packing structures with hexagonal and orthorhombic symmetries. The SC intercellular lipid layers underwent the orthorhombic-to-hexagonal transition at 30-40°C. After decreasing temperature from 40°C to 25°C, small orthorhombic domains with larger lattice constant were formed. The formation of the orthorhombic domains was fairly slow and complicated it proceeded at least two steps. In addition, it seems that the prolonged incubation at 40°C also affects the relaxation process of the hexagonal-to-orthorhombic structural change; the longer the incubation time at 40°C was, the smaller was the intensity of the peak from the orthorhombic domains formed in the first step.

Discussion

These results suggest that the orthorhombic-to-hexagonal transition in the intercellular lipid layers has a complicated temperature hysteresis involving molecular diffusion. Considering that the hexagonal structure formed on heating to 40°C has a smaller lattice constant than that at 20°C and the orthorhombic structures formed on cooling is different from those before heating, these newly formed structures were resulted from the rearrangement of lipid molecules. We will proposed a model for the thermal hysteresis behavior of the orthorhombic-to-hexagonal transition in SC intercellular lipid layers.

References

[1] Pilgram G. S. K., Vissers, D. C., Van der Meulen, J. H., Pavel, S., Lavrijsen, S. P. M., Bouwstra, J. A., Koerten, H. K., Aberrant lipid organization in stratum corneum of patients with atopic dermatitis and lamellar ichthyosis. *J. Invest. Dermatol* 117(2001), 710-717
[2] Hatta, I., Ohta, N., Inoue, K., Yagi, N., Coexistence of two domains in intercellular lipid matrix of stratum corneum. *Biochim. Biophys. Acta* 1758(2006), 1830-1836
[3] Imai, T., Nakazawa, H., Kato, S., Thermal phase transition behavior of lipid layers on a single human corneocyte cell. *Chem. Phys. Lipids* 174(2013), 24-31
[4] Nakazawa, H., Imai, T., Hatta, I., Sakai, S., Inoue, S., Kato, S., 2013. Low-flux Electron Diffraction Study for the Intercellular Lipid Organization on a Human Corneocyte. *Biochim. Biophys. Acta* 1828(2013), 1424-1431

P09

Characterization of Sugar-Bearing Micelles for Targeting Drug Delivery

Mizuha Sakashita[1], Shinichi Mochizuki[1], and Kazuo Sakurai[1,2]

[1]Department of chemistry and biochemistry, The University of Kitakyushu,
1-1 Hibikino, Wakamatsu-ku, Kitakyushu, Fukuoka 808-0135, Japan
[2]CREST, JST Co., Japan
E-mail: t2mab008@eng.kitakyu-u.ac.jp

Introduction

To increase the efficiency in therapeutic gene delivery to target cells, a variety of non-viral vectors has been developed. Sugar bearing lipids are capable of delivering genes to specific cells because there are proteins to recognize the sugar chain structure specifically. Galactose is known to be recognized by asialoglycoprotein receptor (ASGPR) on hepatocytes. In this study, we synthesized a new galactose or glucose bearing lipid (see Fig.1) and examined the recognition ability by the cell.

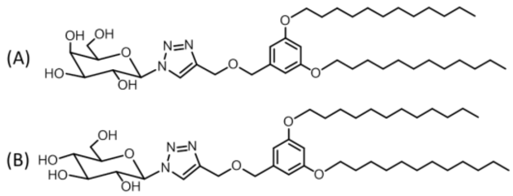

Figure 1. Chemical structure of galactose-bearing lipid (A) and glucose-bearing lipid (B).

Experiments

The complex was prepared by mixing the galactose bearing lipid, DNA and cationic lipid (DOTAP), which was added to make complex with DNA (denoted D_Gal/DNA).We also prepared the glucose one (denoted D_Glc/DNA) and DOTAP was added to make complex with DNA (denoted DOTAP/DNA)as contraol.

We examined the particle sizes of these lipids with the dynamic light scattering (DLS) and the structures of these lipid with the small angle X-ray scattering (SAXS).

We evaluated the recognition ability by the ASGPR, which is a protein that recognizes galactose, with Quarts Crystal Microbalance (QCM). Finally, we examined the gene expression efficiency using HepG2 cells, which are known to have an ASGPR.

Results and Discussions

Fig.2-(A) shows SAXS results of D_Gal/DNA and D_Glc/DNA. These lipids showed the hexagonal diffractions. This result indicates these lipids showed the hexagonal diffractions and were almost equivalent structure.

Fig.2-(B) shows QCM results of the interactions between Gal/DNA or Glc/DNA were injected into the ASGPR. The addition of Gal/DNA induced the decrease of frequency,while that of Glc/DNA and DOTAP/DNA did not. These results indicate that Gal/DNA was recognized by ASGPR. Fig.4 shows the transfection efficiencies by Gal/DNA and Glc/DNA, Lipofectamine2000 (It is commercial cationic lipid) using HepG2 cells. D_Gal/DNA showed the higher transfection efficiency than D_Glc/DNA. This result suggests that the recognition of D_Gal/DNA by parenchymal cells improved the transfection efficiency.

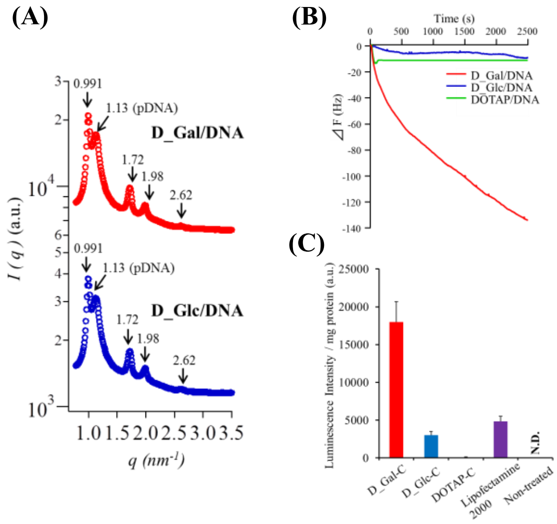

Figure 2. SAXS profiles of the lipoplexes for D_Gal/DNA and D_Glc/DNA (N/P =5) (A). Comparision of ASGPR recognition with QCM (B) and enhanced the transfection(C).

Acknowledgment

This work is financially supported by JST CREST program and all SAXS measurements were carried out at SPring-8 BeamLine40B2 (2012B1252, 2013A1594).

References

[1] Rajesh Mukthavaram, Srujan Marepally, Mahidhar Y Venkata, Gangamodi N.Vegi, Ramakrishna Sistla, Aradinda Chaudhuri, *Science Direct Biomaterials, ELSEVIER*, **2008**,30, 2369-2384

P10

Micellar Structure of an Amphiphilic Alternating Copolymer in Aqueous Medium

Kai Uramoto, Ken Terao, and Akihito Hashidzume, and Takahiro Sato

Department of Macromolecular Science, Osaka University
1-1 Machikaneyama-cho, Toyonaka, Osaka 560-0043, Japan
tsato@chem.sci.osaka-u.ac.jp

Introduction

We have investigated so far various types of amphiphilic polyelectrolytes comprising hydrophobic and ionizable monomer units. Ueda et al.[1] found that the alternating copolymer of sodium maleate and dodecyl vinyl ether [P(MAL/C12), Scheme 1] forms the uni-core flower micelle at the degree of polymerization $N_{0,1}$ less than ca. 300 and multi-core flower necklace at higher $N_{0,1}$. The aggregation number (i.e., the number of copolymer chains) of the flower micelle is inversely proportional to $N_{0,1}$, that is, the number of monomer units per flower micelle is ca. 300 irrespective of $N_{0,1}$. The hydrophobic core of the flower micelle consists of ca. 75 dodecyl groups, and the rest of dodecyl groups attaching to the copolymer chains are out of the core.

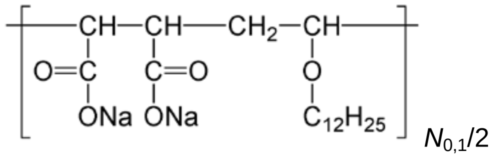

Scheme 1. Chemical structures of P(MAL/C12)

In this study, we have studied local structure of the micelles formed by P(MAL/C12) in 0.025 M aqueous Borax by SAXS.

Results and Discussion

Figure 1 shows scattering functions $I(k)$ for 6 P(MAL/C12) samples with different molecular weights (11k – 330k) in 0.025 M aqueous Borax at 25 °C, obtained using the BL-10C beamline in KEK-PF and the BL-40B2 beamline in SPring-8. The copolymer mass concentration c was fixed to be 1×10^{-3} g/cm^3. All the functions exhibit sharp minimum aroud k (the magnitude of the scattering vector) = 1 nm^{-1}.

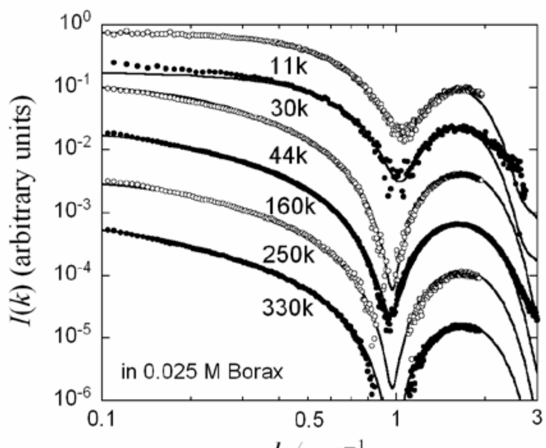

Figure 1. Scattering functions of P(MAL/C12) samples in 0.025 M aqueous Borax at 25 °C

The scattering function $I(k)$ can be calculated from the molar mass M, the particle scattering function $P(k)$, and the second virial coefficient A_2 using

$$I(k) \propto MP(k) \big/ \left[1 + 2A_2 MP(k)c\right]$$

From light scattering results, it turned out that the samples 11k and 30k take the uni-core flower micelle, while the other higher molecular weight samples take the multi-core flower necklace. The particle scattering function $P(k)$ for the flower micelle and flower necklace may be calculated by

$$P(k) = M_{\mathrm{u,w}}{}^{-1} \int M_{\mathrm{u}} P_{M_{\mathrm{u}}}(k) w(M_{\mathrm{u}}) \mathrm{d}M_{\mathrm{u}} \cdot P_{\mathrm{necklace}}(k)$$

where M_{u} and $P_{M\mathrm{u}}(k)$ are the molar mass and the particle scattering function of the unit flower micelle, $w(M_{\mathrm{u}})$ is the distribution function (the weight fraction) of M_{u}, which is characterized by the weight- and number-average molar mass $M_{\mathrm{u,w}}$ and $M_{\mathrm{u,n}}$, and $P_{\mathrm{necklace}}(k)$ is the scattering function of the wormlike nechlace backbone characterized by the persistence length q_{necklace}. ($P_{\mathrm{necklace}}(k) = 1$ for the uni-core flower micelle). Regarding the unit flower micelle as a concentric sphere with the inner and outer radii a and R, respectively, we write $P_{M\mathrm{u}}(k)$ as

$$P_{M_{\mathrm{u}}}(k) = \left[3 \frac{\lambda_{\mathrm{c}} \left(\sin ka - ka \cos ka \right) + \left(\sin kR - kR \cos kR \right)}{\lambda_{\mathrm{c}} \left(ka \right)^3 + \left(kR \right)^3} \right]^2$$

where λ_{c} is the relative excess electron density in the inner sphere over that in the outer sphere, and a and R are calculated from M_{u}.[1]

The solid curves in the figure indicate theoretical values calculated by the above equations using parameters, being consistent with light scattering results. The good agreements between the theory and experiment confirms the previous conclusions[1] on the micellar structure of P(MAL/C12).

1. M. Ueda, et al., Macromolecules, *Macromolecules*, **2011,** 44, 2970.

P11

Analysis of cationic dendrimer's structure using Small angle X-ray scattering

Takuma MINAMI[1], Yusuke SANADA[1,2], Kenshiro NAOYAMA[3], Takuro NIDOME[4], Yoshiki KATAYAMA[3] and Kazuo SAKURAI[1,2]

[1] Engineering Kitakyushu University., 1-1 Hibilino Wakamatsu-ku Kitakyushu Fukuoka 808-0135, Japan,
[2]JST-CREST., K's Gobancho 6F, 7, Gobancho, Chiyoda-ku, Tokyo, 102-0076 Japan,
[3]Kyushu University., 744 Motooka Nishi-ku Fukuoka, 860-8555 Japan
[4] Kumamoto University., 2-39-1 Kurokami Kumamoto, 860-8555 Japan
Address
E-mail: u3mab008@eng.kitakyu-u.ac.jp

Introduction

Dendrimer is dendritic polymer that monomers regularly-branched from core and is classified as 'Generation' by monomer's degree of polymerization. Dendrimers are anticipated to work for Drug Delivery System (DDS) intended to carry the amount necessary to where and when needed medicines . However in research to date , a case of introducing drugs to dendrimers , It is figured out whether the drugs exists in dendrimers or surface dendrimers . Therefore, in this study's purposes is to synthesize the cationic dendrimer and identify the location of drugs in dendrimer-drug complexes. In this poster presentation, I make an announcement about analyzing structure of dendrimer in the way of runup to identifing the location of drugs.

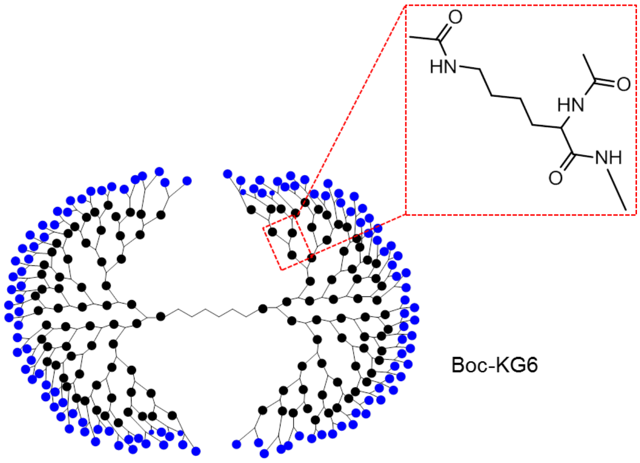

Figure.1 Structure of Generation 6 dendrimer (KG6)

Experiments

We synthesized Generation 4, 5 and 6 denndrimers (KG4, KG5 and KG6). Dendrimer's core is 1,6-Diaminohexane and monomer is L-Lysine protected Boc group. Molecular mass and Structure of the synthesized dendrimers is measured by using Matrix Assisted Laser Desorption / Ionization – Time of Flight Mass Spectrometry (MALDI - TOF MS) and Small angle X-ray Scattering (SAXS).

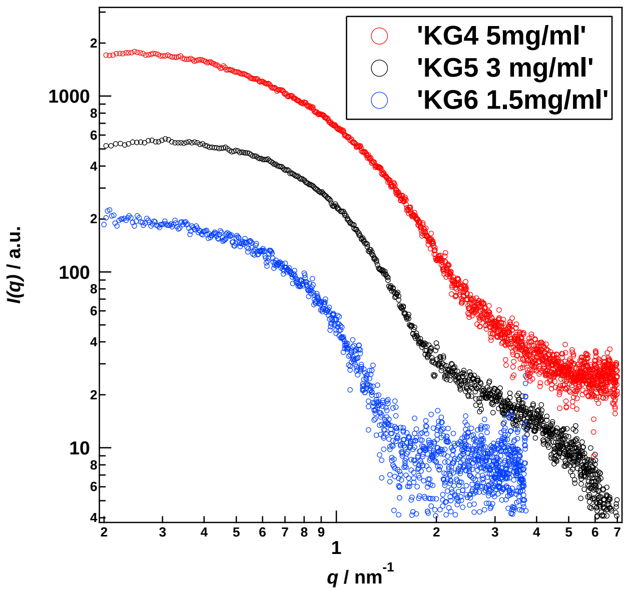

Figure.2 SAXS profile of Generation 4,5 and 6 dendrimar (KG4,5 and 6)

Results and Discussions

Results for MALDI - TOF MS measurement , We confirmed that molecular mass of Generation 4, 5 and 6 dendrimers give close agreement with theoretical value . And results of SAXS measurement , radius of intertia of Generation 5 and 6 denndrimers is 1.54 nm, 1.71 nm and 2.1 nm , respectively and slope of low side found q^0 (Figure. 2) . Slope of low side is q^0 that it means shape of sample is sphere , so we thought structure of Generation 5 and 6 denndrimers is sphere . Therefore, these results show form of dendrimer is spherical and hRadius of intertia size of the higher KG is bigger than that of the lower .

P12

Conformation and Association Behavior of Single-Stranded DNA in Aqueous Solution

Hiroki Yamamura, Keiko Tamada, Ken Terao, and Takahiro Sato
Department of Macromolecular Science, Graduate School of Science, Osaka University
1-1 Machikaneyama-cho, Toyonaka, Osaka, 560-0043, JAPAN
yamamurah11@chem.sci.osaka-u.ac.jp

Introduction

DNA is a biomacromolecule of which monomer consists of the phosphate group and deoxyribose bearing one of four hydrophobic bases (Chart 1). Complementary chains of DNA form a double helix in aqueous solutions. The double helical conformation is stabilized by hydrogen bonds, hydrophobic interactions and stacking interactions between hydrophobic bases,so that dissociated single-stranded DNA chains upon heating easily associate due to bare hydrophobic bases. We investigated the conformation and association behaviour of thermally denatured DNA in dilute aqueous solutions by separation between association components and non-association components using size exclusion chromatography equipped with a multi-angle light scattering on-line detector (SEC-MALS). In addition, we also investigated the local conformation of thermally denatured DNA by ultra violet absorption measurement (UV), circular dichroic measurement (CD) and small angle X-ray scattering (SAXS). In this study, we have compared the association behaviour of a sonicated sample of thermally denatured salmon DNA (S-DNA) and the mixture of poly (deoxyadenosine monophosphate) (PolydA) and poly (thymidine monophosphate) (PolydT) (Chart 2).

Chart 1. Chemical structure of DNA.

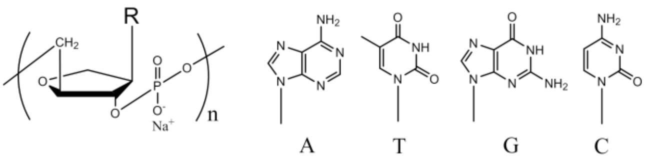

Chart 2. Chemical structures of PolydA and PolydT.

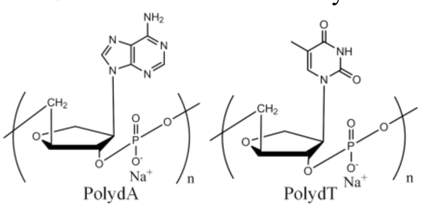

Result and discussion

Figure 1 compares angular dependences of excess X-ray scattering intensities of (a) S-DNA and (b) PolydA+PolydT mixture in 15 mM or 200 mM aqueous NaCl at 25 and 60 ºC. The scattering profile of thermally denatured S-DNA in 200 mM NaCl at 60 ºC (■ in Panel a) is a smoothly decreasing function of *k*, corresponding to the randomly coiled conformation. On the other hand, the profiles of native state S-DNA (○, ● in Panel a) in 200 mM NaCl at 25 and 60 ºC have the peak at scattering vector $k \approx 4.5$ nm^{-1}, which is characteristic to the B-form double helix of DNA When,the thermally denatured S-DNA was cooled down to 25 ºC and 200 mM NaCl was added, the scattering profile (□ in Panel a) has no peak but the shoulder at $k \approx 4.5$ nm^{-1}. This suggests that the B-form double helical conformation is only partly recovered by the denatured S-DNA in 200 mM NaCl at 25 ºC

The scattering profile of PolydA+PolydT in 15 mM NaCl at 60 ºC (● in Panel b) is almost identical with that of denatured S-DNA at 60 ºC (■ in Panel a), indicating that PolydA and PolydT exist as randomly coiled single chains in that solvent condition. On the other hand, intensities of the PolydA + PolydT mixture in both 15 mM and 200 mM aqueous NaCl at 25 ºC (○, □ in Panel b) increase at $k > 6$ nm^{-1}. Zuo et al. proposed the B'- form of the DNA double helix, which exhibits a peak at $k = 7.5$ nm^{-1} as the SAXS fingerprint pattern, which may correspond to the increase of the intensity at $k > 6$ nm^{-1} for PolydA + PolydT mixture at 25 ºC. However, the result for PolydA + PolydT mixture in 200 mM aqueous NaCl at 60 ºC (■ in Panel b) shows the shoulder at $k = 4 \sim 6$ nm^{-1}. This suggests that the associate of PolydA and PolydT takes partly the B-form double helical conformatin, instead of the B'-form, in 200 mM aqueous NaCl at 60 ºC.

In the presentation, the above SAXS results reflecting the local conformation of the associates formed by S-DNA and the PolydA+PolydT mixture are compared with their global conformation.

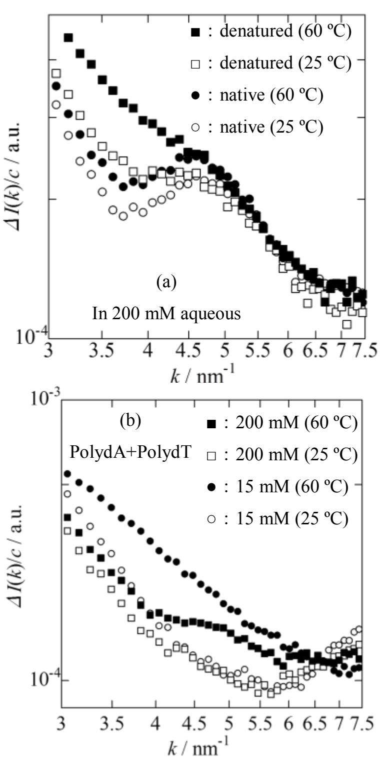

Figure 1: Angular dependences of excess X-ray scattering intensities of (a) S-DNA in 200 mM aqueous NaCl and (b) PolydA+PolydT mixture in 15 mM or 200 mM at 25 and 60 ºC.

Reference

(1) Tamada et al., *Kobunshi Ronbunshu*, **2012**, 69, 399

P13

Local Conformation and Intermolecular Interactions of Rigid Cyclic Amylose Carbamate Derivatives

Ken Terao,[1] Natsuki Asano,[1] Shinichi Kitamura,[2] and Takahiro Sato[1]

[1]Department of Macromolecular Science, Graduate School of Science, Osaka University, 1-1 Machikaneyama-cho, Toyonaka 560-0043, Japan

[2]Graduate School of Life and Environmental Sciences, Osaka Prefecture University, Gakuen-cho, Nakaku, Sakai, 599-8531, Japan

kterao@chem.sci.osaka-u.ac.jp

Cyclic amylose tris(phenylcarbamate) (cATPC) and cyclic amylose tris(n-butylcarbamate) (cATBC) were prepared to obatain rigid ring polymers in solution. Light and small-angle X-ray scattering measurements were made for the samples in some good and Θ solvents to determine mean-square radii of gyration $\langle S^2 \rangle_z$, particle scattering functions $P(q)$, and second virial coefficients A_2 as a function of weight-average molar mass M_w. The obtained data were analyzed in terms of the wormlike ring to determine the molar mass per unit contour length M_L and the Kuhn segment length λ^{-1}. While the obtained M_L and λ^{-1} for cATPC in 1,4-dioxane, 2-ethoxyethanol, and methyl acetate, and cATBC in THF, methanol, and 2-propanol, are substantially the same as those for linear polymer, cATPC in ethyl acetate and 4-methyl-2-pentanone has appreciably larger M_L and smaller λ^{-1}. In these solvents, A_2 at Θ temperature of the corresponding linear polymer are much smaller than the theoretical values calculated in terms of the intermolecular topological interaction, indicating that local helical structure as well as polymer-solvent interactions of cyclic chain are not always the same as the linear analogue.

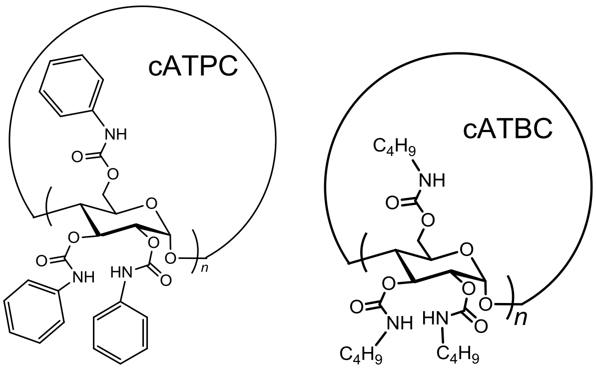

Figure 1. Chemical structures of cyclic amylose tris(phenylcarbamate) (cATPC) and cyclic amylose tris(n-butylcarbamate) (cATBC).

References:

[1] Terao, K.; Asano, N.; Kitamura, S.; Sato, T. *Acs Macro Letters* **2012**, *1*, 1291-1294.

[2] Terao, K.; Shigeuchi, K.; Oyamada, K.; Kitamura, S.; Sato, T. *Macromolecules*, **2013**, *46*, 5355-5362.

[3] Asano, N.; Kitamura, S.; Sato T. *J. Phys Chem. B* **2013**, 117, 9576-9583.

P14

Colloidal Dispersion of a Thermosensitive Block Copolymer in Water

Masaaki Kondo,[1] Kohei Tanaka,[1] Ken Terao,[1] Shinichi Yusa,[2] Takahiro Sato.[1]

[1] Department of Macromolecular Science, Osaka University
1-1 Machikaneyama-cho, Toyonaka, Osaka 560-0043, Japan
kondom12@chem.sci.osaka-u.ac.jp

Introduction

Thermosensitive block copolymers can form self-assemblies upon heating and are expected to be used as the drug delivery system or nano-carrier, Sato et al.[1] investigated the self-association behavior of a thermosensitive amphiphilic block copolymer, poly(*N*-isopropylacrylamide)-*b*-poly(*N*-vinyl-2-pyrrolidone) (PNIPAM-*b*-PNVP; Scheme 1) in water upon heating by combining static light scattering (SLS) and small-angle X-ray scattering (SAXS), and concluded that a liquid-liquid phase separation takes place in the aqueous solution above ca. 40 ˚C, where the concentrated phase exists as colloidal particles of a few hundred size. In this study, we have investigated the temperature dependence of the colloidal particles in aqueous PNIPAM-*b*-PNVP within the biphasic region SLS and SAXS.

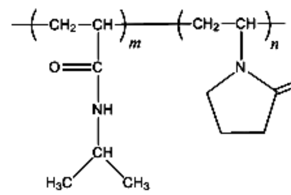

Chart 1. Chemical structure of PNIPAM-*b*-PNVP

Experiment

A $PNIPAM_{100}$-*b*-$PNVP_{218}$ copolymer sample, synthesized by the organotellurium-mediated controlled radical polymerization, was dissolved in water at room temperature (the polymer mass concentration $c = 2 \times 10^{-3}$ g/cm^3). The solution was heated at 60 ˚C and then quenched to 40˚C, and SLS and SAXS measurements were carried out on the solution as a function of time.

Results and Discussion

Figure 1 shows the scattering functions for the aqueous $PNIPAM_{100}$-*b*-$PNVP_{218}$ solution quenched from 60˚C to 40˚C at different times, obtained by SLS and SAXS. Here, R_θ is the excess Rayleigh ratio, K is the optical constant, and k is the magnitude of the scattering vector. The scattering functions decay twice in low and high k regions, indicating that the solution contains polydisperse large spherical particles of the concentrated phase and small star micelles. The height of the second plateau around k = 0.2 nm^{-1} increases with elapsing time, which reflects the increase of the aggregation number for the small star micelle. On the other hand, the aggregation number of the star micelle in the copolymer solution directly heated from the room temperature to 40 ˚C was much smaller than that in the solution quenched from 60 ˚C to 40 ˚C.

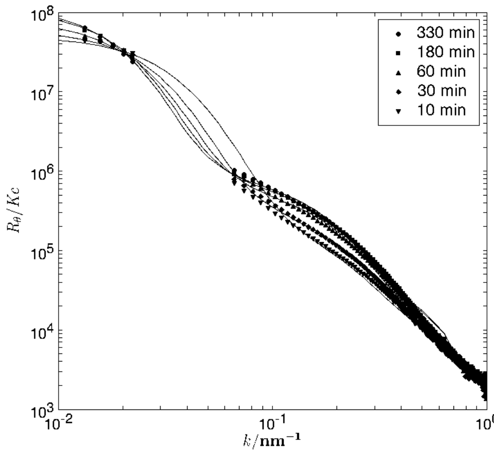

Figure 1. SAXS and SLS profiles for aqueous solutions of $PNIPAM_{100}$-*b*-$PNVP_{218}$ at 3, 60, 180 and 330 min after quenched from 60 to 40˚C.

1. T. Sato *et al.*, *Macromolecules*, **2013**, 46, 226

P15

Temperature changes in molecular conformation and intermolecular interactions of polydialkyl silanes in solution

Xinyue Jiang[1], Ken Terao[1], Woojung Chung[2], Masanobu Naito[2, 3], and Takahito Sato[1]
[1]Osaka University, [2]Nara Institute of Science and Technology, [3]NIMS
1-1 Machikaneyama-cho, Toyonaka, Osaka 560-0043
jiangx11@chem.sci.osaka-u.ac.jp

Introduction

Temperature induced UV absorption spectra change was found for some poly(dialkylsilane)s, which has σ- σ conjugation of the main chain, at low temperature range between −30 and −70 °C.[1] This conformational change of the main chain may influence the chain dimensions as well as the molecular interactions of the polysilanes. However, dimensional properties are hardly measured at such low temperatures in general because of water condensation. Recently, we successfully determined dimensional properties and the second virial coefficient A_2 of polystyrene at −77 ºC by small-angle X-ray scattering (SAXS) measurements with a thermostated nitrogen jet.[2] In this study, SAXS measurements were made for the three polysilane samples shown in Figure 1 to determine the mean-square radius of gyration $\langle S^2 \rangle$ and A_2 in isooctane at a wide temperature range from −77 to 75℃ .

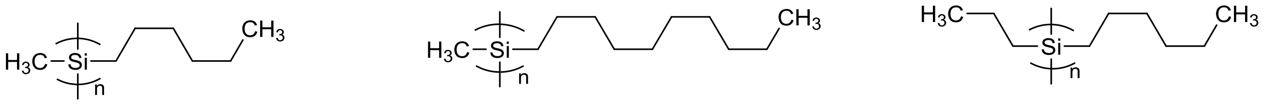

1. PSi1c, $M_w = 3.1\times10^4$ **2.** PSi1d, $M_w = 6.4\times10^4$ **3.** PSi2b, $M_w = 8.4\times10^4$

Figure 1. Chemical structures of poly(*n*-decylmethylsilane) (**1.** PSi1c), and poly(*n*-hexyl-*n*-propylsilane) (**2.** PSi1d), poly(*n*-hexyl-*n*-propylsilane) (**3.** PSi2b).

Results & Discussion

Temperature dependence of maximum absorption wavelength λ_{max} and A_2 is shown in Figure 2. Steep reductions of λ_{max} of PSi1d and PSi2b are observed in between −40 and −70ºC. While the values of $\langle S^2 \rangle$ of the polysilane samples do not depend significantly on the temperature, A_2 of PSi1d and PSi2b decreases sharply with lowering temperature around −50℃ and negative A_2 were observed at lower temperatures, indicating that the polymer-polymer interactions become attractive with the conformational change.

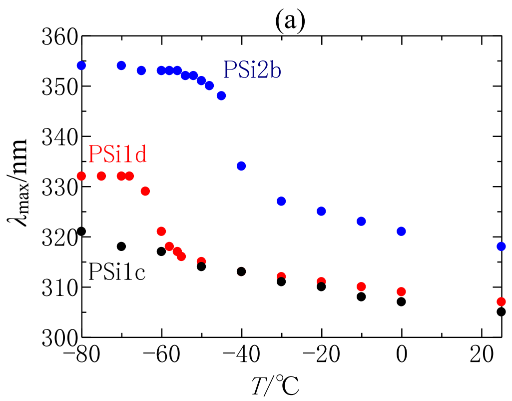

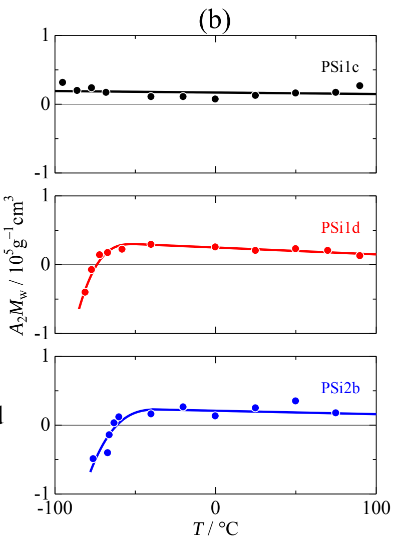

Figure 2. Temperature-dependent λ_{max} (a) and A_2 (b) of PSi1c, PSi1d, and PSi2b.

References: 1) W. Chung, H. Shibaguchi, K. Terao, M. Fujiki, and M. Naito, *Macromolecules*, 44, 6568-6573 (2011), 2) K. Terao, N. Morihana, and H. Ichikawa, *Polym. J.*, in press.

P16

Mannose-bearing Micelles for Targeting DDS and its Structure

Ichiki Fukuda[1], Mizuha Sakashita[1], Shinichi Mochizuki[1],Kazuo Sakurai[1,2] （university of kitakyushu[1],JST-CREST[2]）

[Introduction]

In gene therapy, carrier is required safety and the capability to carry DNA for medical treatment. For example, non-virus carrier is safer than virus carrier and it has the ability as a carrier. Especially the lipids bearing the sugar chain is useful as a career since there are proteins to recognize specific sugar chain structure. Mannose can expect specific gene delivery because mannose is recognized by mannose receptor exists in a macrophage. In this study, we synthesized the lipids bearing mannose in a hydrophilic group (Man-lipid) newly, and we will try gene delivery to a target cell using these lipids.

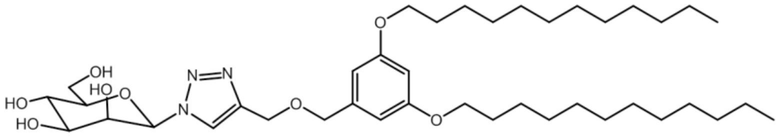

Fig.1 Chemical structure of Man-lipid

[Experiment]

DNA is known to be interacting with cationic lipid. To prepare the complex with DNA, we mixed Man-lipid and DOTAP which is commercial cationic lipid to 1:1 (denoted D_Man). It was investigated by small angle X-ray scattering (SAXS) whether Man-lipid and DOTAP, or D_Man and DNA would have made the complex. Moreover, we performed agarose gel electrophoresis to observe whether DNA and D_Man would made complex, and we considered N/P ratio.

[Result and Discussion]

The result of SAXS measurement was shown in Fig.2. Although only a form factor appears in a DOTAP, the structure factor has appeared in D_Man. It suggests that the internal structure of D_Man is hexagonal packing. As mentioned above, Man-lipid and DOTAP can made the complex. SAXS profile of D-Man, structure factor appears similarly and the internal structure is hexagonal packing like D_Man.The result of agarose gel electrophoresis was shown in Fig.3. It turned out that D_Man and DNA can made complex completely by 2 in the N/P ratio. This complex is formed by a low N/P ratio. Much mannose can be included it. Therefore, it may have the high selectivity to a macrophage.

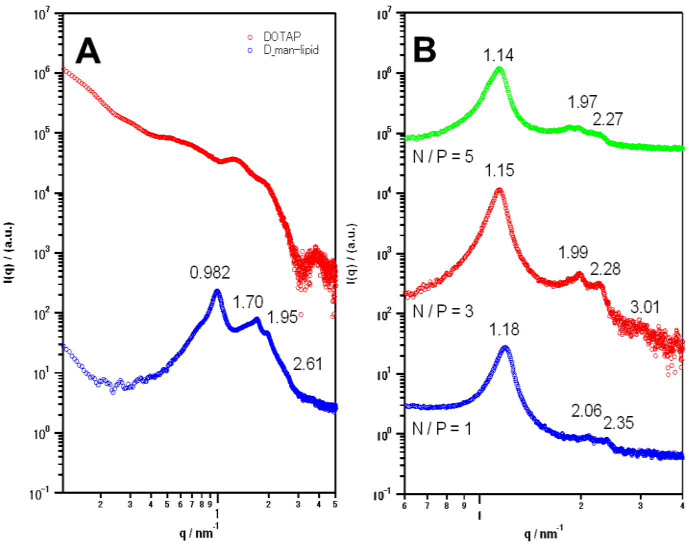

Fig.2 (A) SAXS spectrum of DOTAP and D_Man (B) SAXS spectrum of DNA complex

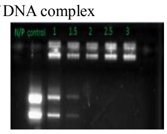

Fig.3 agarose gel electrophoresis

P17

Orientation and Distribution of Intercellular Lipid Domains in Pig Stratum Corneum

Shiori Kakinoki, Shiho Arai, and Hirohisa Yoshida

Graduate School of Urban Environmental Science, Tokyo Metropolitan University
1-1, Minami-Osawa, Hachioji, Tokyo 192-0397 JAPAN
kakinoki-shiori@ed.tmu.ac.jp

Introduction

Transportation of water in the outermost layer of skin, stratum corneum (SC) is the important subject from the medical and health care viewpoints. The intercellular lipid matrix forms the stable structure with water content between 20 and 30 wt% in SC [1-3]. Three kinds of water exsist in SC such as non-freezing, boud and free waters by thermal analysis [4,5]. Water molecules show the concentaration gradient in the *in vivo* SC and the staday state in the *ex vivo* SC [3]. In this study, the orientation and distribution of intercellular lipds in the *ex vivo* pig SC were investigated by GISAXS, GIWAXS and AFM.

Experiments

Pig SC supplied from Japan Charles River Co Ltd. was used for the experiment without further purification. setting on silicon wafer using a spin coated Aron Alpha (dry SC). SC on Si wafer was hold in the relative humidity 98% for 24 hrs (wet SC). The water content of dry and wet SC was 7 and 22 %, respectively. The diffusion process of deuterium oxide (D_2O) in pig SC was investigated by the deuterium-hydrogen exchange using FTIR.

Grazing incidence small and wide angle X-ray scattering experiments were carried out at FSBL03XU, SPring-8, JASRI, Japan. The wave length of X-ray was 0.1 nm, the incident angle was 0.15°, the distance between sample and the ditectore (R-Axis and CCD) was 2328 mm. The cross sectional observation of SC was carried out by AFM (Atomic Forth Microscopy; Hitachi Hitech Co. ltd, E-Sweep) uting a canti lever (43 N/m) at 338 kHz.

Results and Discussions

The diffusion process of D_2O in SC was divided to three steps, adsorption and diffusion in surface layer and inside SC. The diffusion coefficient of D_2O was 0.0016 – 0.0027 cm^2/h obtained by FTIR. These values showed a good agrrement to the diffusion coefficient of water in the swelling process of short lammellar evaluated by GISAXS methods.

GISAXS images of dry and wet SC are shown in Fig. 1. The first and second order diffraction peaks of short lammellar and the third order diffraction peak of long lammellar were observed in the out-of plane direction for dry SC. No diffraction peak was observed in the in plane direction. The long and short lammellars stacked parellel to the SC surface with few ditribution. For wet SC, all diffraction peaks of long and short lammellars became clear and those intensity increased. The fourth diffraction peak of short lammellar was observed for wet SC. The order of long and short lammellars increased with the abosorption of water.

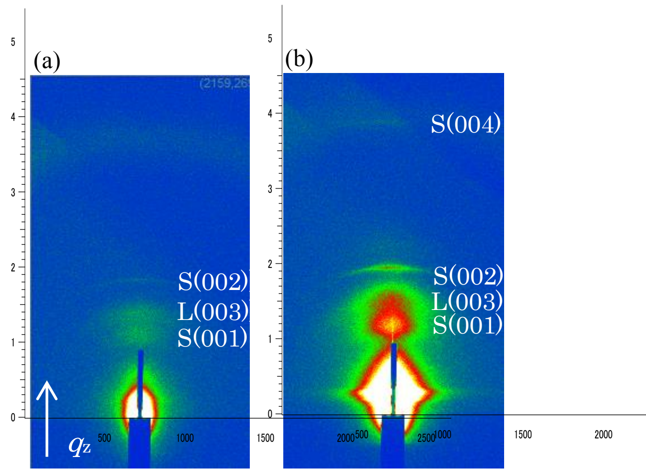

Fig.1 GISAXS image of dry SC(a) and wet SC(b)

The cross sectional view of dry SC was observed by AFM, in which the corneocytes were embedded in the intercellular lipid matrix. The location of long and short lamellar domains was evaluated. The short lamellar domains surrounding corneocytes acted as a water transportation path in SC.

1. J. A. Bouwstra etal, *J. Invest. Dermatol*., 120, 750 (1994)
2. N. Ohta etal, *Chem. Phis. Lipids*, 123, 1 (2003)
3. H. Nakazawa etal, *Chem. Phis. Lipids*, 165, 238 (2012)
4. K. Walkley, *J. Invest. Dermatol*., 59, 225 (1972)
5. G. Imokawa etal, *J. Invest. Dermatol*., 96, 845 (1991)

P18

Analysis of Structural Change in pH-responsive Polymer Micelle with Anomalous Small angle X-ray scattering

Masaki Kinoshita, Aya Okura, Daisuke Kugimoto, Isamu Akiba
Department of Chemistry and Biochemistry, The University of Kitakyushu, Kitakyushu, Japan
1-1, Hibikino, Wakamatsu-ku, Kitakyushu, Fukuoka 808-0135, Japan
E-mail: u3maa003@eng.kitakyu-u.ac.jp

Introduction

Polymer micelles with responsiveness for external stimuli, such as temperature or pH, are keenly investigated to create soft-materials with autonomy. When polymer micelles are composed of block copolymers having polyelectrolytes as hydrophilic chains, they should show pH-responsive structural change triggered by pH-responsive change of conformation of corona chain. Therefore, the polymer micelles having polyelectrolytes as corona chains are expected to be pH-responsive polymer micelles. Thus, in this study, we investigate pH-responsive structural change of polymer micelle composed of amphiphilic block copolymers having polyelectrolyte as a hydrophilic chain by combination of small-angle X-ray scattering (SAXS) and anomalous SAXS (ASAXS).

Experimental

As the pH-responsive amphiphilic brock copolymer, poly(methacrylic acid)-*block*-poly(2-bromoethyl methacrylate) (**Poly1**) was synthesized with sequential RAFT method. Micelle solutions at various molar ratios of NaOH to COOH of poly(methacrylic acid) ([NaOH]/[COOH]) were prepared by solvent displacement method. Also, measurement sample was prepared micelle solution was diluted with NaOHaq. SAXS and ASAXS near Br *K*-edge measurements for **Poly1** micelles were carried out at BL40B2 station of SPring-8 in Japan. In ASAXS measurements, 13.373, 13.423, and 13.468 keV were used as the energies of incident X-ray.

Result and discussion

Fig. 1 show the energy resonant terms ($V^2(q)$) of **Poly1** micelles near Br *K*-edge. $V^2(q)$ profiles are drastically changed with [NaOH]/[COOH]. At [NaOH]/[COOH] = 0, $V^2(q)$ profile of the micelles shows good agreement with the theoretical curve calculated for spherical micelle. On the other hand, when 0 < [NaOH]/[-COOH] ≦ 1, $V^2(q)$ shows q^{-2}-dependence at low q. This suggests that shape of hydrophobic core drastically changes in association with conformational change of corona chains.

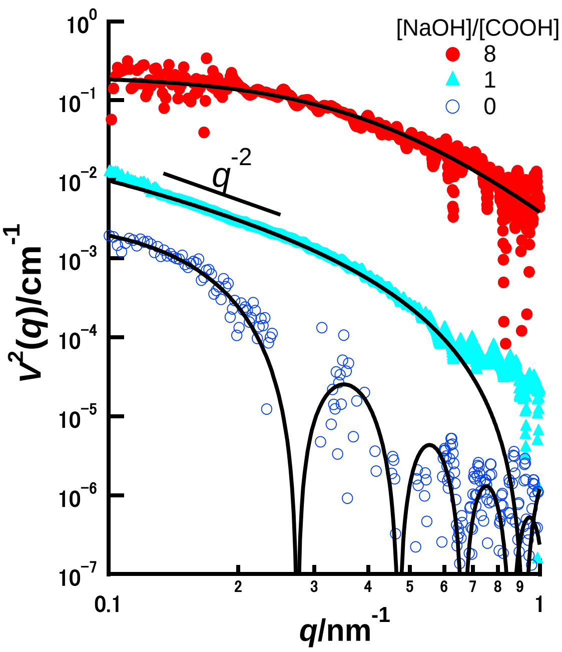

Fig. 1. ASAXS profiles of Poly1 micelle in neutral and alkaline aqueous solution.

Methionine adsorption on Au nanoparticle surface fabricated by solution plasma method compared with cysteine adsorption

Shinya YAGI[1,2], Chie TSUKADA[3], Toyokazu NOMOTO[4], Galif KUTLUK [2], Hirofumi NAMATAME[2], and Masaki TANIGUCHI[2]

[1]EcoTopia Science Institute, Nagoya University, [2]Synchrotron Radiation Center, Hiroshima University, [3]Graduate School of Engineering, Nagoya University, [4]Aichi Synchrotron Radiation Center
Furo-cho, Chikusa-ku, Nagoya, 464-8603 Japan
s-yagi@nucl.nagoya-u.ac.jp

Introduction

For the application to medical materials, it is important to reveal a mechanism of adsorption reaction between an amino acid molecules, which is a component of protein, and a metal nanparticles (NPs). The NPs must have a bio-compatibility for our body against an allergy reaction. From the point of a bio-compatibility view, therefore, the understandings of the adsorption reaction are needed from both medical and medicine fields. When the metal NPs are ingested into the living body, we are focusing on the amino acid molecules. Since the adsorption reaction between sulfur and transition metal is to be a very unique, the understanding the changing of the chemical state of the sulfur atom of amino-acid molecule is important. In our previous study, we have paid attention to the reaction between L-cysteine [$HSCH_2CH(NH_2)COOH$] and the Au NPs surface [1]. Thus, we have selected L-cysteine and L-methionine [$H_3CSCH_2CH(NH_2)COOH$], which are including sulfur atom, in this study. The L-cysteine has chemisorbed on the Au NPs surface and decomposed to the thiolate structure. Judging from this result, it is thought that the S-H bond is dissociated easily compared with the S-C bond. In this study, we have focused to the adsorption reaction of the L-methionine amino acid and the Au NPs under water environment, and investigated by sulfur K-edge NEXAFS measurement with He-path system.

Experimental

The Au NPs in aqueous solution were fabricated by the solution plasma method [2]. This fabrication method did not use any surfactant molecule. The starting materials were a distilled water (milli-Q (≥18.3 MΩcm)), NaCl(electrolyte) and Au rods (electrode). The average diameter of the fabricated Au NPs was estimated to be about 5-10 nm. The L-methionine powder (>98 %, Katayama Chemical) of 0.05 mmol was dissolved into the Au NPs colloidal solution of 2 mL at room temperature. The S K-edge NEXAFS was carried out by fluorescence X-ray yield method using the atmospheric XAFS measurement system with He-path at the BL-3 in HiSOR [3]. The fluorescence yield detection was employed using a gas-flow type proportional counter with P-10 gas (10 % CH_4 in Ar). The incident X-ray energy was calibrated on the assumption that the first peak of K_2SO_4 appeared at 2481.7 eV.

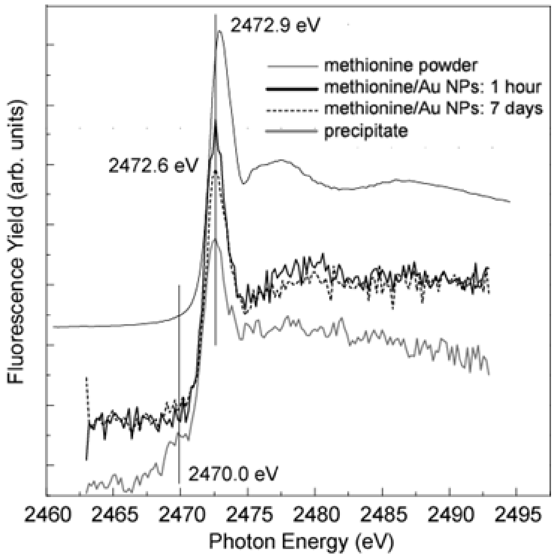

Figure 1. S K-edge NEXAFS spectra for methionine powder, methionine/Au NPs and precipitate.

Results and discussion

Figure 1 shows the sulfur K-edge NEXAFS spectra for methionine powder, methionine reacted with the Au NPs under water environment for 1 hour and 7 days, and precipitate. A strong peak located at 2472.9 eV for the methionine powder sample means the transition from sulfur 1s to the antibonding σ^*(S-C) molecular orbital. On the other hand, A peak for the methionine reacted with the Au NPs is shifted slightly to lower photon energy side of 0.3 eV. Moreover, the peak intensity for the specimen after 7 days is decreased in comparison with that of after 1 hour. These results indicate that the methionine molecules adsorb on the Au NPs surface by a weak chemical bonding and a small amount charge is transferred from the Au NPs to the antibonding σ^*(S-C) molecular orbital. A small peak located at 2470.0 eV for the precipitate means the chemical state of the atomic sulfur on the Au NPs surface. This indicates that some of adsorbed methionine molecules dissociates into the atomic sulfur after long reaction time.

References

[1] C. Tsukada, S. Yagi, T. Nomoto, T. Mizutani, S. Ogawa, H. Nameki, Y. Nakanishi, G. Kutluk, H. Namatame, M. Taniguchi, *Appl. Surf. Sci.*, **262**, 231 (2012).
[2] H. Nameki, *private communication in Aichi Prefectural Technical Report* (2010).
[3] Shinya YAGI, *Houshako*, **18**, 316 (2005).

Adsorption reaction between biomolecules and gold nanoparticles prepared by solution plasma method

Chie TSUKADA[1], Takuma TSUJI[1], Koichi MATSUO[2], Toyokazu NOMOTO[3], Galif KUTLUK[2], Masahiro Sawada[2], Hirofumi NAMATAME[2], Masaki TANIGUCHI[2], Tomoko YOSHIDA[4] and Shinya YAGI[2,4]

[1]Graduate School of Engineering, Nagoya University, [2]Synchrotron Radiation Center, Hiroshima University, [3]Aichi Synchrotron Radiation Center, [4]EcoTopia Science Institute, Nagoya University
Furo-cho, Chikusa-ku, Nagoya, 464-8603 Japan
tsukada.chie@e.mbox.nagoya-u.ac.jp

Introduction

A range for nanoparticles (NPs) use has been expanded in recent years. For example, the NPs are indispensable in the chemical synthesis and the automotive industries. On the other hand, in the medical viewpoint, researches on drug delivery systems and biocompatibility have been paid attention. When the NPs are applied to a living body, it is important to note the starting materials used to preparation of the NPs. Though reducing agent and surfactant reagents are used to inhibit the aggregation of the NPs each other in preparing the NPs, we think that such reagents poison the living body. Therefore, it is necessary to prepare the NPs without using those reagents. Nameki et al. have reported that Au NPs can be prepared from three starting materials, which are water, electrolytes and gold rods, with plasma under water solution environment [1]. This method is called the solution plasma method. In that preparation method, the electrolyte indicates NaCl or KCl, and the gold rods are used as a electrode. When the Au NPs are ingested into the living body, we are focusing on the adsorption reaction between Au NPs and the L-cysteine or the phosphatidylcholine(PC) molecules. It is because we are thinking of two things. One is that the cysteine exists in abundance as a free amino acid molecule in the body. The other one is that the cell membrane surface is constructed of mainly PC molecules. Thus we have selected two biomolecules of the L-cysteine and PC as reaction molecules, respectively. In this study, we have investigated the adsorption reaction between those biomolecules and the Au NPs prepared by the solution plasma method using soft X-ray synchrotron light.

Experimental

The Au NPs colloidal solution was prepared by the solution plasma method [1-3]. The average diameter of the prepared Au NPs is estimated to be approximately 5-20 nm. The PC powder (Egg, >99 %) was added into the milli-Q water (≥18.3 MΩcm) and stirred by the vortex. The PC suspension or L-cysteine powder (≥98 %) was added into the Au NPs colloidal solution. When the adsorption reactions were promoted, the black colored precipitates occurred. The precipitates were rinsed with milli-Q water to remove the molecules un-adsorbed on the Au NPs. The P K-edge NEXAFS was carried out by fluorescence X-ray yield method using the He-path system with the silicon drift detector (SDD) at BL-6N1 in Aichi SR. The S K-edge NEXAFS was carried out by fluorescence X-ray yield method using the atmospheric XAFS measurement system with He-path at the BL-3 in HiSOR [4]. The fluorescence yield detection was employed using a gas-flow type proportional counter with P-10 gas (10 % CH_4 in Ar). The incident X-ray energies were calibrated on the assumption that the first peak of $FePO_4$ and K_2SO_4 appeared at 2153.0 eV and 2481.7 eV, respectively.

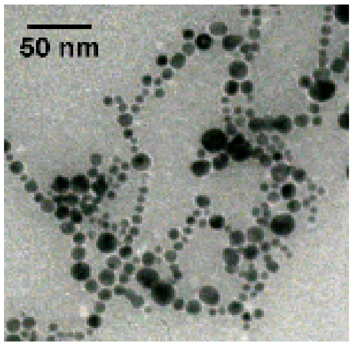

Figure 1. TEM image of the Au NPs precipitate prepared by negative staining method.

Results and discussion

Figure 1 shows the TEM image of the Au NPs precipitate prepared by negative staining method. The contrast of the Au NPs surface is bright slightly. In addition, we have revealed that the Au NPs adsorb on the surface of liposome membrane constructed with the PC molecules [5]. Thus, it is speculated that the PC molecule adsorbs on the Au NP surface. The P K-edge NEXAFS spectra before/after adsorption reaction of the PC molecule with the Au NPs show that the Au NPs surface is covered with the chemisorbed PC molecule, because the peak intensity originated from the PC molecule decreases after the adsorption reaction. On the other hand, the L-cysteine adsorbs chemically on the Au NPs surface at thiol part [6]. The adsorbate form is cysteine thiolate. When the adsorption reaction has been promoted, the different spectrum component suggesting another adsorbate is observed. This component possesses a shoulder structure and is located at 2473.0 eV. That peak position shows a presence of the cystine molecule. Those results mean that the cystine has been synthesized from the adsorbed cysteine on the Au NPs surface under water environment.

References

[1] H. Nameki, private communication in Aichi Prefectural Technical Report (2010). [2] T. Mizutani et al., *Thomson Reuters database* (2012). [3] X. Hu et al., *Cryst. Growth Des.*, **12**, 119 (2012). [4] S. Yagi, *Houshako*, **18** (2005) 316. [5] C. Tsukada et al., *submitted to J. Surf. Anal.* (2013). [6] C. Tsukada et al., *e-J. Surf. Sci. Nanotech.* **11** (2013) 18.

P21

Anomalous diffusion of polystyrene grafted nanoparticles dispersed in polystyrene matrix studied by X-ray photon correlation spectroscopy

T. Hoshino[1,2], D. Murakami[1,2], S. Ogawa[1,2], Y. Tanaka[2], M. Takata[2], H. Jinnai[1,2], A. Takahara[1,2]
[1]JST, ERATO Takahara Softinterfaces, [2]RIKEN/SPring-8
[1]CE80, Kyushu University, 744 Motooka, Nishi-ku, Fukuoka 819-0395, Japan
[2] RIKEN SPring-8 Center, 1-1-1 Kouto, Sayo, Hyogo 679-5148, Japan
E-mail: t-hoshino@cstf.kyushu-u.ac.jp

Introduction

Study of dynamical behavior of colloids or nanoparticles (NPs) is considerably important for nano-medicine such as drug delivery systems. Although the dynamical behavior of NPs in polymer matrix is different from that of the normal Brownian motion, the details of such dynamical behavior are still unknown. Moreover, the dynamical features of polymer-grafted NPs are rarely studied. In the present study, the dynamics of the polystyrene (PS)-grafted NPs dispersed in PS matrix were studied using X-ray photon correlation spectroscopy (XPCS).

Experiment

The silica NPs (110 nm in diameter) grafted with PS brushes (M_n = 2.30×10^4, M_w/M_n=1.41, and 0.28 chains nm^{-2}) were dispersed in the PS matrices. In order to investigate the effect of the chain length of the polymer matrix, two different samples were prepared: the one with molecular weight of the matrix (M_n = 1.05×10^4, M_w/M_n=1.09, and T_g=367 K, where T_g is the glass transition temperature) being smaller than that of brushes (sample-A), while the other with the molecular weight of the matrix (M_n = 3.00×10^4, M_w/M_n=1.06, and T_g=374 K) being larger than that of brushes (sample-B).

An XPCS instrument, using a fast pixel array detector PILATUS with the grid mask resolution enhancer, has been installed at the BL19LXU beamline of SPring-8 [1]. In an XPCS measurement, samples are coherently illuminated, and the fluctuation of scattered speckle intensity is observed. The time-autocorrelation functions, $g_2(q,t)$, are then calculated from the fluctuation, where q and t are the wave vector and time, respectively.

Results and Discussions

Figure 1 shows the representative $g_2(q,t)$ for sample-A at q=2.15×10^{-2} nm^{-1} over the investigated temperature, T, range between 433 K and 503 K. The solid lines are the best-fit curves with the stretched (or compressed) exponential equation, $g_2(q,t)= A \exp[-2(\Gamma t)^{\beta}]+1$, where A, Γ and β ($\neq$1) are a contrast, relaxation rate, and stretched (or compressed) exponent, respectively. $\beta \neq 1$ means that the NP behavior was different from normal Brownian motion.

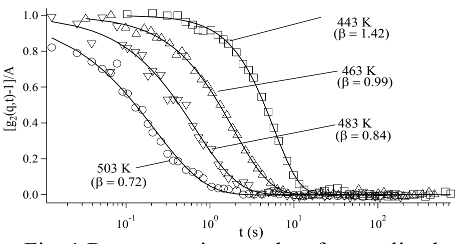

Fig. 1 Representative results of normalized time-autocorrelation functions at q=2.15×10^{-2} nm^{-1} of the scattered speckle intensity from PS-grafted NPs in PS matrix of sample-A at differemt temperatures. Solid lines are fitted curves by stretched exponential function.

In order to understand the NP behavior on a microscopic scale, the experimental data were analyzed with a kind of continuous time random walk (CTRW) model [2]. In the CTRW model, the particle motion is expressed by discrete steps. The mean displacement of a particle after N steps is expressed by $N^{\alpha}\delta$, and the mean elapsed time by $N\tau_0$. Here, δ is the average length of a single jump and τ_0 is the mean time between the jumps. Brownian motion is described by α = 0.5, whereas α > 0.5 and α < 0.5 correspond to, respectively, hyperdiffusive and subdiffusive behavior. From the fitting analysis of the measured $g_2(q,t)$ with the CTRW model at each temperature, although α = 0.8 was obtained at T = 433 K, α decreased with increasing temperature, and reached below 0.5 at $T \approx$ 457 K, which is 1.25T_g, and finally dropped to α = 0.3 at T = 503 K. Thus the NPs behavior of sample-A changes from hyperdiffusive motion to subdiffusive motion at 1.25T_g [3].

On the other hand, in the case of sample-B, although α > 0.5 was also obtained at T < 1.25T_g, α = 0.5, corresponding to the normal Brownian motion, was obtained at T > 1.25T_g. The different dynamical behaviors between the two samles at T > 1.25T_g should come from the difference of the chain length of the matrix. That may be explained as follows: In the case of sample-A, the shorter chains of the matrix chains than that of the brushes wet the brushes, and so the interaction between the matrix chains and the brushes causes subdiffusive motion of the NPs. In contrast, in the case of sample-B, the longer matrix chains do not wet the brushes, therefore, the much less interaction between the matrix and brushes allows the NPs to move like the normal Brownian motion.

[1] T. Hoshino et al., *J.Synchrotron Rad.*, **19**, 988 (2012). [2] Duri et al., *Europhys. Lett.* **76**, 972 (2006).
[3] T. Hoshino et al., *Phys. Rev. E.*, **88**, 032602 (2013).

P22

Structure analysis of associating structure of amphiphilic AB_n-type polymer with small-angle X-ray scattering

Daisuke Kugimoto, Aya Okura, Masaki Kinoshita and Isamu Akiba
Department of Chemistry & Biochemistry, The University of Kitakyushu, Kitakyushu, Japan
1-1, Hibikino, Wakamatsu-ku, Kitakyushu, Fukuoka 808-0135, Japan
E-mail: u3maa004@eng.kitakyu-u.ac.jp

Introduction

Polymer micelles composed of amphiphilic block copolymers are affected by molecular architectures of constituent polymers. In case of star-shaped amphiphilic block copolymer composed of one hydrophobic chain and some hydrophilic chains, hydrophilic chains are crowded at core-shell interface. Therefore, it is considered that effect of crowding of hydrophilic chains on micelle formation is significantly appeared in comparison with linear block copolymer [1]. Thus, investigation of the effect of crowding at core-shell interface in star-shaped amphiphilic block copolymer on structure of polymer micelle is of great interest. In this study, we investigated associating behavior of star-shaped amphiphilic block copolymer (AB_n-type polymer) having one hydrophobic A chain and n hydrophilic B chains.

Experimental

Series of star-shaped amphiphilic block copolymer (AB_n-type polymers, n = 1~3) composed of stearyl chain (C18) as A chains and poly(ethylene glycohol) (PEG) as B chain were synthesized in two conditions. One condition is total volume of PEG chains is the same, the other condition is length of PEG chains is the same. These polymer micelle solutions were prepared by dissolve these polymers in water. (1 mg/mL)

Structure of these micelles are analysed with dynamic light scattering (DLS), small-angle X-ray scattering (SAXS) and field-flow fractionation with multi-angle light scattering (FFF-MALS) measurement.

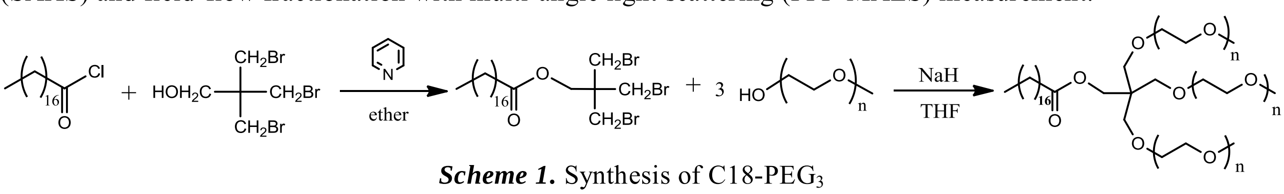

Scheme 1. Synthesis of C18-PEG_3

Result and discussion

Fig. 1 shows SAXS profiles of C18-PEG_n micelles. As a result of core-shell sphere model fitting in this SAXS profiles, were reproduced accurately all profile. Therefore, these polymer micelle structure is spherical shape. In addition, SAXS measurements indicate that size of micelles decreases with increasing n of AB_n-type polymers. This result is consistent with DLS results. Further, the aggregation number measured by FFF-MALS for the micelles is inevitably decreased with increasing n. This means that the increment of number density of hydrophilic PEG chains increases the curvature of core-shell interface of the micelles. Therefore, it is considered that the curvature of the core-shell interface of micelles is altered to sustain optimal number density of PEG chain at the interface.

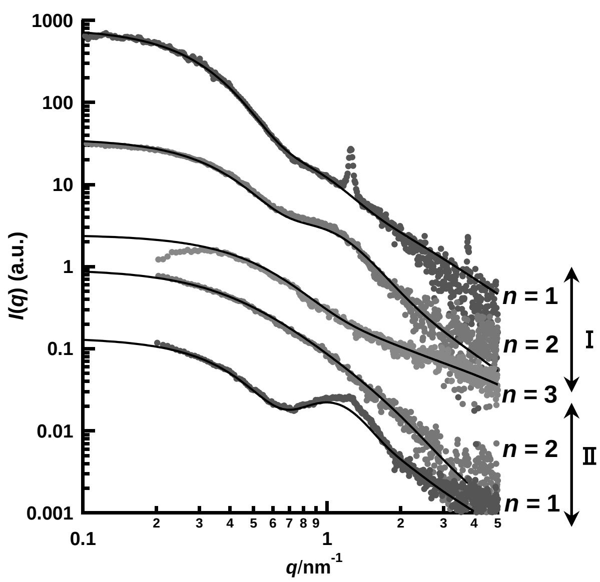

Fig. 1. SAXS profiles of micelles of C18-PEG_n.
Ⅰ: volume of PEG chain condition is the same,
Ⅱ: length of PEG chain condition is the same.

Reference

[1] Sanada, Y.; Sakamoto, S.; Akiba, I.; Takaki, T.; Sakurai, K. *Chem. Lett.* **2013**, *42*, 882-884.

Upgrade and Promotion of Industrial Use of Small Angle X-ray Scattering Beamlines at the Photon Factory

Hideaki Takagi[1], Nobutaka Shimizu[1], Noriyuki Igarashi[1], Takeharu Mori[1], Shinya Saijo[1], Hiromasa Ohta[2], Ai Kamijo[1], Masanori Komuro[1], Masaharu Nomura[1]

[1]Photon Factory, High Energy Accelerator Research Organization
[2]Mitsubishi Electric System & Service Co., Ltd
Address
E-mail address: takagih@post.kek.jp

Introduction

High flux beam generated by the synchrotron radiation is widely used in various scientific fields in both basic and applied study. The Photon Factory (PF) is the Japanese synchrotron facilities and has been utilized more than 30 years. Small angle X-ray scattering (SAXS) is a powerful tool for material science and biological science. SAXS is used for the large hierarchical structural analysis from nanoscale to microscale on the basis of such the structural information as averaged particle size, shape and distribution. Recently, grazing-incidence small angle X-ray scattering (GISAXS) measurement has been developed as an appropriate method to investigate nanoscale structure of various kinds of materials on surface or interface in thin-films and functional membranes. Moreover, GISAXS in the soft-X-ray region (SX-GISAXS) is a new technique to examine nanoscale structure near surface. SX-GISAXS might promote the depth-sensitive analysis in the direction perpendicular to the substrate by tuning the angle and the energy of the incident beam.

Upgrade of SAXS Beamlines at the PF

There are two SAXS beamlines, BL-6A (old BL-15A) and BL-10C [1, 2] at the PF. A great number of achievements have been accomplished in material and biological science for over 30 years. We recently started improvement and the advancement of these beamlines in order to improve the ease of operation and support the latest experimental techniques. The new long diffractometers and the high-speed and the large area hybrid pixel detectors, PILATUS3 1M and 2M (Dectris) will be installed in BL-6A, BL-10C, respectively. We are basically going to reconstruct all the components of BL-10C in next March. A fix-exit double crystal monochrometer will be newly installed to tune X-ray energies from 6 keV to 14 keV. A new bent-cylindrical mirror and a bender system will be also installed, and the focusing ratio will be increased to make the beam brilliance higher than the present. The new SAXS beamline, BL-15A2, was constructed in this autumn [3]. The light source of BL-15A2 is a short gap undulator which produces high brilliance X-ray beam from 2.1 keV to 15 keV. A SX-GISAXS diffractometer and a 3.5 m-length long diffractometer will be tandemly installed in the experimental hutch, and the highly collimated brilliance beam is available at the each focusing point. Moreover, three PILATUS3 detectors for a wide-angle X-ray scattering (WAXS) will be also installed in each beamlines, and the simultaneous SAXS/WAXS system will be constructed with two PILATUSs.

These advancements will refurbish the activities of the SAXS fields at the PF. Therefore, we now promote not only the academic use but also the industrial and manufacturing application with SAXS techniques. In this presentation, we introduce the upgrade of SAXS beamlines and the effort to industrial application program [4] at the PF.

[1] N. Igarashi, Y. Watanabe, Y. Shinohara, Y. Inoko, G. Matsuba, H. Okuda, T. Mori and K. Ito, J. Phys.: Conf. Ser. 272 (2011) 012026
[2] N. Shimizu, T. Mori, N. Igarashi, H. Ohta, Y. Nagatani, T. Kosuge and K. Ito, J. Phys.: Conf. Ser. 425 (2013) 202008.
[3] N. Igarashi, N. Shimizu, A. Koyama, T. Mori, H. Ohta, Y. Niwa, H. Nitani, H. Abe, M. Nomura, T. Shioya, K. Tsuchiya and K. Ito, J. Phys.: Conf. Ser. 425 (2013) 072016.
[4] http://pfwww.kek.jp/innovationPF/

P24

Application of SR-XRF and XAFS for the trace element analysis contained in histopathological specimens

Motohiro Uo[1], Takahiro Wada[1], Tomoko Sugiyama[2], Mikio Kusama[2], Daisuke Omagari[3]
Kazuo Komiyama[3], Natsuko Taniguchi[4], Takashi Inomata[4], Satoshi Konno[4], Masaharu Nishimura[4]

[1]Advanced Biomaterials Section, Tokyo Medical and Dental University
[2] Department of Dentistry, Oral & Maxillofacial Surgery, Jichi Medical University
[3] Department of Pathology, School of Dentistry, Nihon University
[4] First Department of Medicine, School of Medicine, Hokkaido University
uo.abm@tmd.ac.jp

Introduction Various metallic materials are widely used for medical and dental materials. Erosion and mechanical wearing of those materials placed in the human body have been reported to be associated with localized and systemic problems. Especially, the oral and the respiratory mucosae are exposed to various dental restorative materials and inhaled airborne debris. The analysis of foreign objects in tissues is important in determining the diagnosis. However, the histopathological specimens are specific to each case and patient. Therefore, the elemental analysis should be carried out non-destructively. In this study, SR-XRF and XAFS methods were applied for the analyses of trace elements and foreign objects contained in the histopathological specimens without damaging.

Materials and Methods The paraffin embedded histopathological specimens of lung and oral mucosae were sliced in 8μm-thickness and placed over the Kapton® film (12.5μm in thickness) and applied for XRF and XAFS analyses. In case of lung biopsy specimens, dried tissues were also applied for those analyses. SR-XRF analyses were carried at BL-4A of KEK-PF and BL37XU of SPring-8. For the typically localized elements, XAFS analysis was carried to reveal the chemical state of the target elements. XAFS analysis was carried at BL-4A, 9A and NW-10A of KEK-PF.

Results and Discussions Cemented tungsten carbide (WC) is widely used for cutting tools because of its high hardness, while, the inhaled fine debris generated during the working with cemented WC cause severe problem called "tungsten carbide pneumoconiosis". For the definite diagnosis of the WC pneumoconiosis, the detection of small amount of WC in the lung biopsy specimens is required. Fig.1 shows the XRF spectra of the dried lung biopsy specimens. Clear fluorescent X-ray assigned for W L series were observed from two specimens obtained from different part of lung. Fig.2 shows W L_1-edge XANES spectra of those specimens and the chemical state of W contained in those specimens was identified as WC. Thus, the caused material of this case could be diagnosed as the inhaled WC. The elemental distribution images of W in the sliced paraffin embedded histological specimen was also successfully obtained using microbeam SR-XRF and W was observed near the surface of the plumonary alveolus. Oral mucosal specimens of the oral lichenoid legion (OLL) were also estimated. A part of OLL is suggested to be related with the eroded metallic ions from the dental restorations. In the SR-XRF measurements, typical components of dental alloys, e.g. Ag, Pd, Au, Cu, Zn, were clearly detected and their localization could be visualized as the distribution images using the thin sliced paraffin embedded specimens. Thus, the affect of the dental alloys to OLL was suggested with the elemental analysis using SR-XRF. In this study, the applicability of SR-XRF and XAFS for the elemental and chemical state analyses using ordinary histopathological specimens was suggested. The paraffin embedded specimen is widely used for the ordinary pathological diagnosis and easily available. Therefore, those methods would be applicable for the diagnosis of various lesions.

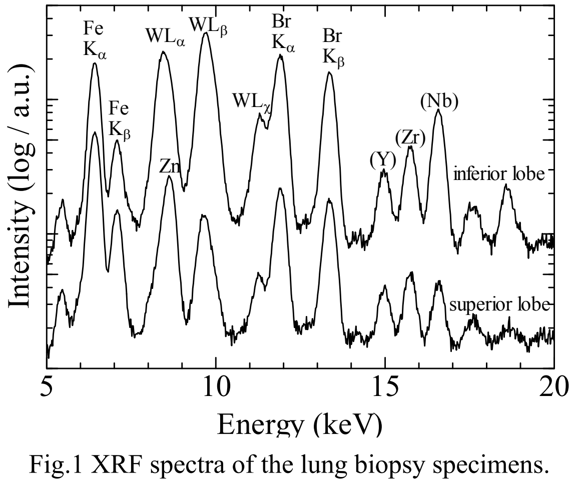

Fig.1 XRF spectra of the lung biopsy specimens. (incident X-ray=30keV)

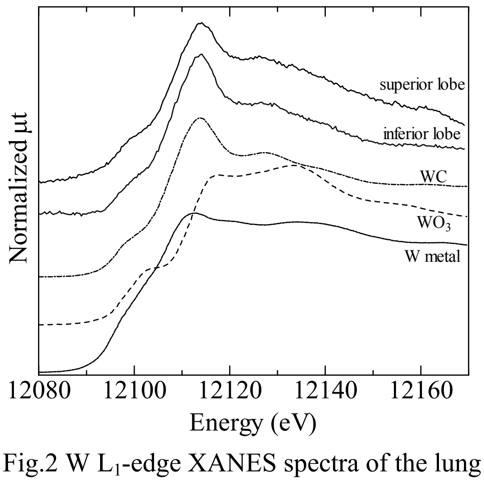

Fig.2 W L_1-edge XANES spectra of the lung biopsy specimens and standards.

Influence of alkyl chain length of calix[4]arene-based cationic lipid for transfection efficiency

Koichi Nishina[1], Shota Fujii[1], Shinichi Mochizuki[1], and Kazuo Sakurai[1, 2]

[1]The University of Kitakyushu, [2]CREST, JST Co., Japan
Hibikino Wakamatsu-ku, Kitakyushu, Fukuoka 808-0135, Japan
t2mab014@eng.kitakyu-u.ac.jp

Introduction

Drug Delivery System (DDS) is expected to be useful to cure diseases like gene disorders. There are two types of DDS carriers. They are virus carrier and non-virus carrier. Recently non-virus carrier was studied because virus carrier has infection disease. Cationic lipid (CL) is one of non-virus carriers. A variety of gene carriers using cationic lipids has been studied. Among them, multivalent cationic lipids are known to show better gene expression efficiency. We synthesized calix[4]arene-based cationic lipids with different alkyl chain length (C3, 6, 9, 12, 15, Fig.1) and evaluated relationship between the alkyl chain length and the transfection efficiency.

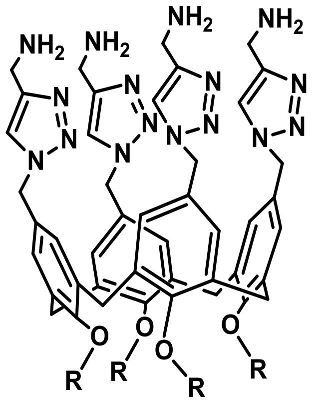

R

C_3H_7 : C3

C_6H_{13} : C6

C_9H_{19} : C9

$C_{12}H_{25}$: C12

$C_{15}H_{31}$: C15

Fig.1 The chemical structure of calix[4]-arene lipids

Experiments

We made DNA/CL complex to add the plasmid DNA encoding luciferase to CL at N/Pratio = 3. The size and structure of the complex were measured by dynamic light scattering (DLS) and small angle X-ray scattering (SAXS). A549 cells were transfected using the complex, and we measured luciferase expression.

Results and Discussion

SAXS measurements showed lamella structures for all complexes. The peaks in figure2 showed that the surface separation between lamella, the spacing of each complexes is equal to the alkyl chain lengths. DNA/C6 complexes showed the highest transfection efficiency among all complexes. DNA/C9 and C12 complexes showed the second and third efficiency, respectively. All complexes showed low cytotoxicity, and same cellular uptake. Importantly, release of plasmid DNA from a mimicked endosome was dependent on alkyl chain length. We supposed that the stability of complexes with long alkyl chain lengths is higher than it with short alkyl chain length. We found that the transfection efficiency is strongly influenced by the ability to release DNA from the complex.

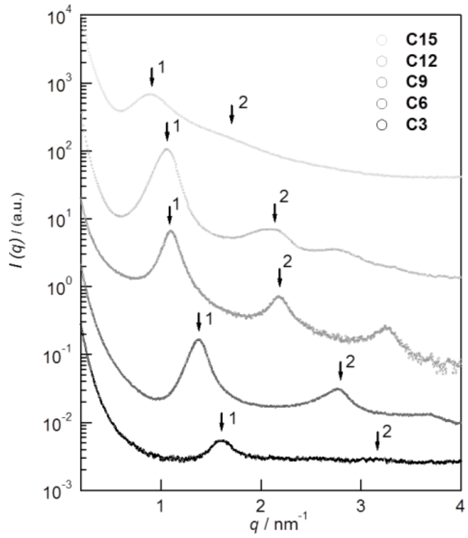

Fig.2 SAXS profiles of the lipoplexes for CaL[4]Cn; C3, C6, C9, C12, C15 (N/Pratio = 2).

RIKEN Small Angle X-ray Scattering Beamline (BL45XU) at SPring-8

Takaaki Hikima[1], Hiromi Sato[1], Hiroyasu Masunaga[1,2], Sono Sasaki[1,3], Naoto Yagi[1,2], and Masaki Yamamoto[1]

[1]RIKEN SPring-8 Center, [2]JASRI/SPring-8, [3]Kyoto Institute of Technology
[1]1-1-1, Kouto, Sayo-cho, Sayo-gun, Hyogo 679-5148, JAPAN, [2]1-1-1, Kouto, Sayo-cho, Sayo-gun, Hyogo 679-5198, JAPAN, [3]Matsugasaki, Sakyo-ku, Kyoto 606-8585, JAPAN

hikima@spring8.or.jp

Introduction

RIKEN BL45XU equipped with tandem undulators consists of two experimental stations: small-angle X-ray scattering (SAXS) and small- and wide-angle X-ray scattering (SWAXS) (Figs 1 and 2). Both equipment can be independently carried out. The beamline was constructed in 1997 for SAXS and protein crystallography. SWAXS station was reconstructed from PX station in 2009.

Area of research

SAXS-station: Time-resolve structures of non-crystalline biological materials such as protein, nucleic acid solutions, membrane, and micelle system under various conditions, are studied by using small-angle scattering and diffraction technique.

SWAXS-station: Wide-scale structural analysis for nano- and meso-structure in soft-condensed matters such as polymer, lipid and complex fluid systems are investigated by using small- and wide-angle X-ray scattering and diffraction techniques.

In this poster, we will introduce some equipment, such as solution scattering system, GISAXS, and micro-beam, and results of research at BL45XU.

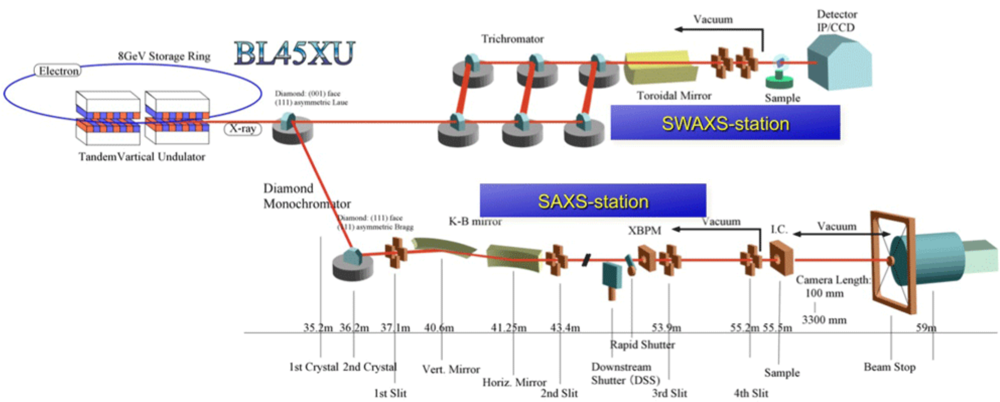

Figure 1. Optics of BL45XU.

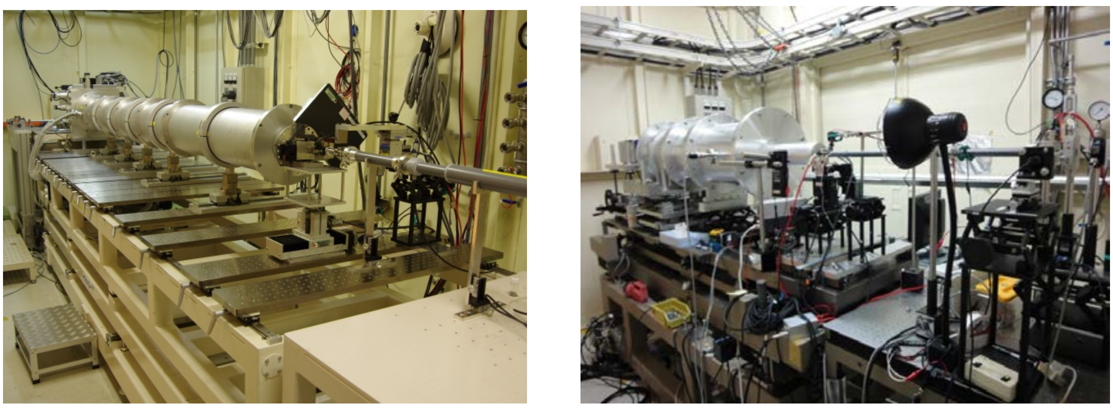

Figure 2. BL45XU SAXS station (left) and SWAXS station (right).

P27

Induced Circular Dichroism for Suger Appended Calixarene Micelles.

Shunsuke SAKAMOTO[1], Yusuke SANADA[1], and Kazuo SAKURAI[1,2]

[1]The University of Kitakyushu, [2]JST-CREST
[1]1-1 Hibikino, Wakamatsu-ku, 808-0135 Kitakyushu, Fukuoka, Japan.
E-mail: t2mab009@eng.kitakyu-u.ac.jp

Introduction

Chiral amplification is one of the most important phenomena in asymmetric synthesis and is researched actively in supramolecular chemistry. Specifically, calixarene is useful as building block for amphiphilic compounds and we synthesized several calixarene derivatives.
(Fujii, S, et al, 2011, Langmuir)

We found that by the addition of achiral calixarene with four amines as achiral head group, named CaL3(Fig1a), to achiral micelles which contain chiral calixarene which has four galactoses as chiral head group, named Gal(Fig.1b), circular dichroism induction was occurred in aqueous media. However Gal shows its own CD of negative sign at 217 nm for its intermolecular chirality in molecularly dispersed solution, the induced CD has positive sign and observed at 237 nm. It suggests that the origin of the CD induction is related with the structural change of Gal/CaL3-complexes.

Experiments

We performed Small Angle X-ray Scattering (SAXS) and Transmission Electron Microscope (TEM) observation to clarify the mechanism of this newly CD induction.

Next, to reveal this unique CD induction, we synthesized L-Galactose-bearing calix [4] arene lipid and performed CD measurement.

Results and Conclusion

From SAXS and TEM results, Gal forms bilayer micelles in aqueous solution and Gal/CaL3-complexes takes fiber-shaped structure twisted. It is thought that this twisted-shape is the origin of induced CD at 237 nm. We think about the mechanism of CD induction that Gal's symmetric bilayer micelles has no structural chirality in spite of the chirality of Gal, but when the micelle transformed into twisted-fiber shaped one by addition of achiral CaL3, attached chiral sugar group affects the direction of twist of micelle.

From CD result, CD spectra of D-gal and L-Gal are line symmetry. It suggests that newly induced CD reflects optical activity of Galactose.

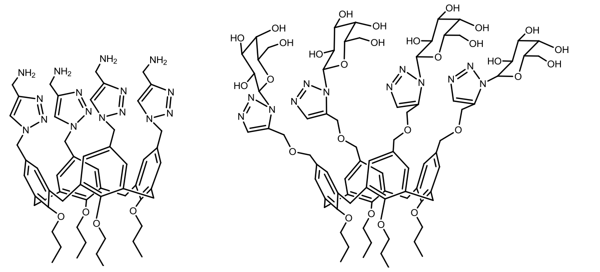
a: CaL3 b: Gal

Fig.1 a: Chemical Formula of Amine-bearing Calix[4]arene
b: Chemical Formula of Galactose-bearing Calix[4]arene

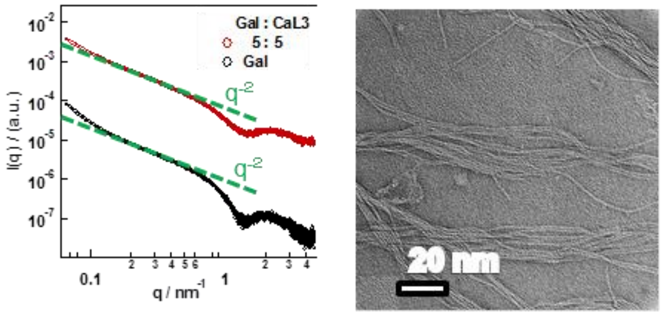

Fig.2 SAXS profiles of Gal and Gal/CaL3 complex, and TEM

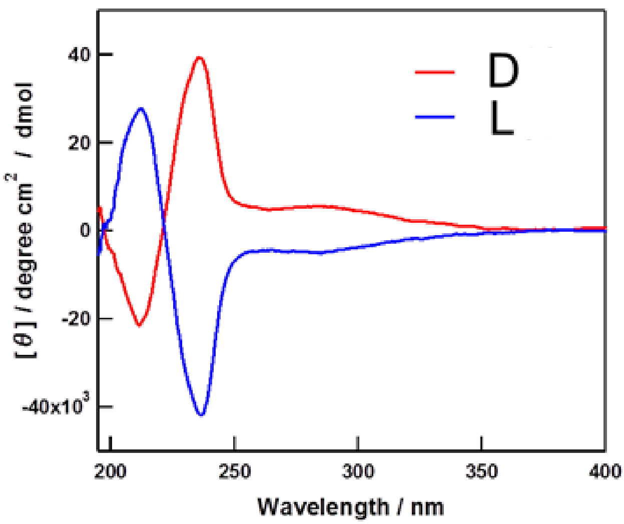

Fig.3 CD Spectra of D-Gal and L-Gal